The European Journal of Finance

ISSN: (Print) (Online) Journal homepage: www.tandfonline.com/journals/rejf20

The dynamics of price jumps in the stock market: an empirical study on Europe and U.S.

Fabrizio Ferriani & Patrick Zoi

To cite this article: Fabrizio Ferriani & Patrick Zoi (2022) The dynamics of price jumps in the stock market: an empirical study on Europe and U.S., The European Journal of Finance, 28:7, 718-742, DOI: 10.1080/1351847X.2020.1740288

To link to this article: https://doi.org/10.1080/1351847X.2020.1740288

THE EUROPEAN JOURNAL OF FINANCE
2022, VOL. 28, NO. 7, 718–742
https://doi.org/10.1080/1351847X.2020.1740288

The dynamics of price jumps in the stock market: an empirical study on Europe and U.S.

Fabrizio Ferriani[a] and Patrick Zoi[b]

[a]DG for Economics, Statistics and Research, Banca d'Italia, Rome, Italy; [b]Economic Research Unit, Trieste Branch, Banca d'Italia, Rome, Italy

ABSTRACT

We study the bivariate jump process involving the S&P 500 and the Euro Stoxx 50, with jumps extracted from high-frequency data. In our analysis, based on Hawkes processes, we find no evidence of contagion across different markets. Nevertheless, we observe significant jump clustering effects though they are limited to intraday time scales. Moreover, we notice that the relative contribution of jumps to the total price variance is larger during tranquil market conditions rather than in periods of stress, providing empirical evidence of this result during the subprime mortgage crisis and the European sovereign debt crisis. Importantly, our results are robust under different jump detection methods.

ARTICLE HISTORY
Received 2 February 2019
Accepted 18 February 2020

KEYWORDS
Jumps; contagion; Hawkes process; high-frequency data

JEL CLASSIFICATIONS
C32; C58; G15

1. Introduction

Prices of traded assets are sometimes subject to sudden movements which cannot be generated by continuous processes, such events are commonly named '*Jumps*'. They are often associated with a sudden flow of new information (Bajgrowicz, Scaillet, and Treccani 2016), though there is no general consensus on the nature of the events that can generate such abrupt price reactions. Merton (1976) first introduced price jumps in his seminal paper, starting an extensive strand of literature in asset pricing and financial econometrics. As highlighted by Ait-Sahalia (2004), the study of jumps is extremely relevant for investors, risk managers, and regulators from several perspectives. Jumps and stochastic volatility can both generate fat tails in the distribution of asset returns with a significant impact on the value-at-risk (VaR), though only jumps can produce fat tailed and skewed distributions over short time scales (see for instance Duffie and Pan 2001). Achieving a decomposition of the ultimate source of risk is therefore crucial for risk management purposes. For option pricing, discontinuities in the price paths are also extremely relevant because the replicating portfolio argument of Black and Scholes (1973) fails when the market is incomplete as the jump risk cannot be perfectly hedged. The impact of jumps on implied volatilities and risk premia is widely documented in the literature (see Duffie, Pan, and Singleton 2000; Eraker, Johannes, and Polson 2003; Wright and Zhou 2009; Bollerslev and Todorov 2011 among others). Important implications for asset allocation problems are extensively discussed by Liu, Longstaff, and Pan (2003) and Aït-Sahalia, Cacho-Diaz, and Hurd (2009).

In this paper, we study the bivariate jump process involving the S&P500 and the Euro Stoxx 50 indexes that are representative of two leading stock markets. We contribute to the literature studying the relevant features of the jump process such as jump clustering and transmission across different world markets. Few recent papers investigate jumps at the multivariate level and they mostly focus on their simultaneous occurrence on multiple stocks within the same market (co-jumps): Bollerslev, Law, and Tauchen (2008) develop a specific test for

CONTACT Patrick Zoi patrick.zoi@bancaditalia.it

pairwise jump detection, Gilder, Shackleton, and Taylor (2014) analyze co-jumps in the US market, Caporin, Kolokolov, and Renò (2017) develop a new test for simultaneous jumps on multiple stocks to investigate systemic events, Bormetti et al. (2015) study the systemic diffusion of jumps among the most liquid Italian stocks. While co-jumps can occur on assets that are traded simultaneously, Aït-Sahalia, Cacho-Diaz, and Laeven (2015) (ADL henceforth) argue that jumps can also transmit across world markets with a time lag and they use multivariate Hawkes processes to capture this form of 'contagion'. Departing from the approach of ADL, relying on a fully parametric model estimated on daily data, we extract jumps from high-frequency data and then we use Hawkes processes to model their dynamics. Surprisingly, we find completely different results: no evidence of jump transmission across markets while self excitation effects are statistically significant but they are detectable only at intraday time scales (compatibly with Bajgrowicz, Scaillet, and Treccani 2016 who find no effects over different trading days). Moreover, the number of jumps detected during low-volatility periods and their contribution to the total price variance are higher than in period of stress (e.g. the subprime and the European sovereign crisis). This is also a fundamental difference with the dynamics entailed in the model of ADL, where price jumps characterize periods of market turmoil. In our case such periods are instead dominated by large volatility fluctuations that can be hardly distinguished from jumps at the daily time scale. To improve the accuracy of our analysis, we allow the jump activity to depend on the level of volatility using the generalized version of the Hawkes process proposed by Bowsher (2007). Our estimates show a strong inverse dependence that can be at least partially related to an increasing difficulty of disentangling jumps from diffusion when the volatility is higher. Importantly our results are robust under different jump identification methods.[1]

The implications of our empirical findings are extremely relevant for risk management and option pricing. If jumps were to propagate across markets, as argued by ADL, then a jump in one market could significantly change the conditional distribution of returns in other markets due to contagion risk. Unlike the model of Merton (1976), jump risk could not be easily differentiated and rational investors would reasonably require a risk premium to face contagion risk; finally, the specific implications of contagion in asset allocation problems are exhaustively discussed in Ait-Sahalia and Hurd (2015).

The rest of this paper is organized as follows. Section 2 describes the data and Section 3 reviews the most common approaches for jump identification. Section 4 presents the multivariate Hawkes framework which is adopted to model the asset price dynamics, while Section 5 concludes.

2. Data description

Our data set comes from Olsen data and contains information on the S&P 500 and the Euro Stoxx 50 indexes between 2007-09-13 and 2014-04-30; the two indexes are traded at the NYSE and at the Frankfurt Stock Exchange, respectively. The 7-year period covered by our analysis includes the subprime crisis, leading to the bankruptcy of Lehman Brothers on September 15th 2008 and the subsequent European sovereign crisis in 2011. For both markets, we compute the total return from prices reported every 5 minutes. This frequency is widely recognized to offer a reasonable balance between a fine sampling frequency on the one hand and robustness to market microstructure noise on the other (see for instance Andersen et al. 2010). The NYSE and the Frankfurt Stock Exchange normally operate respectively form 9:30 to 16:00 and from 9:00 to 17:30 in local times. The first price is observed 5 minutes after the opening time. Each ordinary trading day has respectively 77 intraday returns for the S&P 500 and 100 returns for the Euro Stoxx 50. For the latter we ignore the first 10 minutes of activity due to a remarkably higher price variability compared to the rest of the day. This choice aims at minimizing the impact of the erratic price behavior often induced by market opening procedures, an approach similar to Gilder, Shackleton, and Taylor (2014). We also exclude from the data set an extremely small set of days containing an anomalous number of price observations, such as those where markets are open for half a session only. At the end of the data cleaning process, our sample consists of 1674 trading days for the S&P 500 and 1691 for the Euro Stoxx 50. The cumulated log-return and the intraday annualized volatility measured from high-frequency returns are reported in Figure 1 where we can observe the highest volatility peaks during the subprime and the Euro Sovereign crisis.

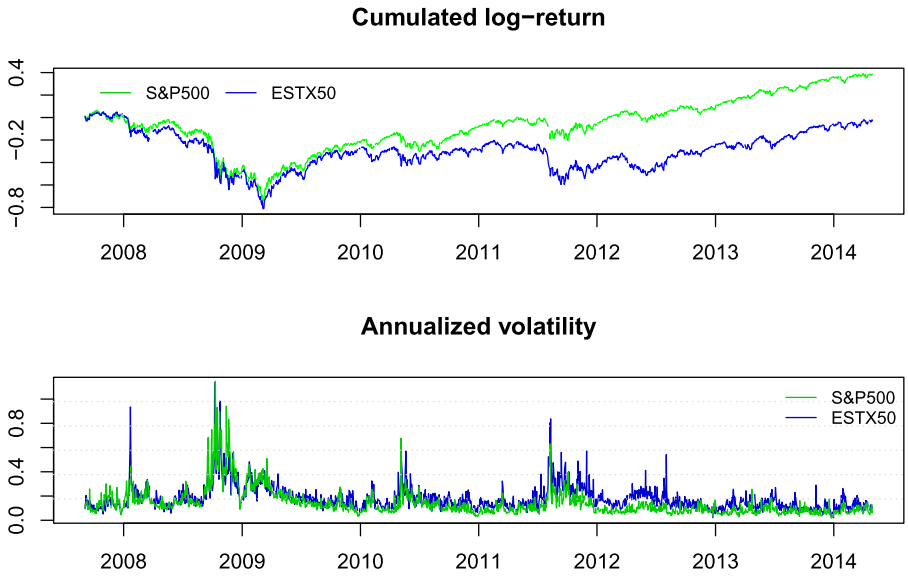

Figure 1. The top panel exhibits the time series of cumulated log-returns (including the overnight period). The bottom panel reports the time series of the annualized volatility.

3. Jumps identification

In recent times, the study of price jumps has largely benefited from the increasing availability of high-frequency data fostering a copious scientific production in the field of jump detection. Seminal contributions include Barndorff-Nielsen and Shephard (2004), Barndorff-Nielsen and Shephard (2006) (BNS henceforth), Huang and Tauchen (2005), Andersen, Bollerslev, and Diebold (2007b), Andersen et al. (2010). To summarize the most relevant studies on jump identification techniques, we conveniently distinguish two main families.

The first one is the BNS family which includes all the tests that relies on the comparison between two realized measures of volatility: the bipower variation and the quadratic variation. The former is driven exclusively by continuous price changes while the latter also includes jumps. Afterwards, several alternative tests have been proposed based on different volatility measures that are also robust to jumps: Mancini (2009) suggests a threshold-based estimator, Corsi, Pirino, and Renò (2010) (CPR henceforth) introduce a thresholded version of the bipower variation (BNS), while Andersen, Dobrev, and Schaumburg (2012) develop new measures based on the nearest neighbor truncation. Christensen, Oomen, and Podolskij (2010) introduce quantile based estimators that generalize the latter approach, being also robust to market microstructure noise. The second important family has been introduced by Lee and Mykland (2008) (LM henceforth) and is based on the idea that jumps can be identified when a return exceeds a certain threshold that is determined adaptively based on the instantaneous volatility. The proposals of Andersen, Bollerslev, and Diebold (2007b), Bollerslev, Todorov, and Li (2013) and Bormetti et al. (2015) belong to the LM family and they differentiate on the methodology employed to determine the volatility and the threshold level.

Unfortunately, none of the available identification methods is generally preferred to the others, with studies showing that the performances of the various tests in finite samples are related to the features of the data generating process as well as to the time frequency of prices observations (see Dumitru and Urga 2011; Gilder, Shackleton, and Taylor 2014 among others). For this reason, we conduct our analysis under three different detection methods selecting one test from the BNS family, one test from the LM family, and a third set of jumps derived as the intersection of the previous two. According to Dumitru and Urga (2011), the intersection of two jump tests generally leads to a substantial reduction of the effective size compared to the nominal one. In the following we first describe the families of non-parametric tests for jump identification, then we present both descriptive and graphical evidence on the jumps occurrence in the two markets.

3.1. Jump tests

Assume, as usual, that prices follow a continuous-time semi-martingale and let the log-price p_t be described by the stochastic differential equation

$$p_t = \int_0^t \mu_s \, \mathrm{d}s + \int_0^t \sigma_s \, \mathrm{d}W_s + \int_0^t J_s \, \mathrm{d}N_s \tag{1}$$

where the drift μ_t has finite variation, the volatility σ_t is càdlàg, W_t is a standard Brownian motion, N_t is a finite activity counting process with possibly stochastic intensity λ_t and J_t is the random jump size. The stochastic processes encompassed by Equation (1) exclude infinite jump activity. However, the class of models covered is widely recognized to be flexible enough to capture the main features of financial time series at high-frequency (see for instance Andersen, Bollerslev, and Dobrev 2007a; Andersen et al. 2010).

Assume also that each trading day t has duration 1 and $M+1$ log-prices $p_{t,0}, \ldots, p_{t,M+1}$ are observed at equally spaced times. The intraday log-returns are indicated as $r_{t,i} = p_{t,i+1} - p_{t,i}$ for $i = 1, \ldots, M$ or alternatively with a single index r_i to denote the ith log-return in the entire time series: $i = 1, \ldots, M \cdot T$ where T is the total number of trading days.

3.1.1. The BNS family of tests

The following volatility metrics is essential to the computation of the test statistics:

$$RV_t = \sum_{i=1}^{M} r_{t,i}^2 \tag{2}$$

RV_t is the realized variance that converges in probability to the quadratic variation as $M \to \infty$:

$$p \lim_{M \to \infty} RV_t = QV_t = \int_{t-1}^{t} \sigma_s^2 \, \mathrm{d}s + \int_{t-1}^{t} J_s{}^2 \, \mathrm{d}N_s \tag{3}$$

and in absence of jumps the quadratic variation corresponds to the integrated variance:

$$QV_t = IV_t = \int_{t-1}^{t} \sigma_s^2 \, \mathrm{d}s \tag{4}$$

To separate the contribution to the realized variance due to continuous price variation from the contribution of jumps, BNS introduce the bipower variation:

$$BPV_t \equiv \mu_1^{-2} \left(\frac{M}{M-1} \right) \sum_{i=2}^{M} \left| r_{t,i-1} \right| \left| r_{t,i} \right| \tag{5}$$

where $\mu_\gamma = \mathbb{E}(|u|^\gamma)$ and $u \sim N(0,1)$. In the asymptotic limit

$$p \lim_{M \to \infty} BPV_t = \int_{t-1}^{t} \sigma_s^2 \, \mathrm{d}s$$

moreover, in absence of jumps, under other regularity conditions, the joint asymptotic distribution of RV_t and IV_t is normally distributed

$$\sqrt{M} \begin{pmatrix} RV_{t,M} - IV \\ BV_{t,M} - IV \end{pmatrix} \xrightarrow{D} N \left(0, \begin{bmatrix} 2 & 2 \\ 2 & 2.62 \end{bmatrix} IQ_t \right) \tag{6}$$

where $IQ_t = \int_{t-1}^{t} \sigma_s^4 \, ds$ is the integrated quarticity. BNS propose some alternative statistics to compute the test, the most common being based on the relative jump measure:

$$RJ_t \equiv \frac{RV_t - \hat{IV}_t}{RV_t} \tag{7}$$

where $\hat{IV}_t$ denotes some jump robust measure of the integrated variance. We generally define the test statistics for BNS family as

$$Z_t \equiv \frac{RJ_t}{\sqrt{\frac{1}{M}\left(\nu_{\hat{IV}_t} - \nu_{RV_t}\right)\frac{\hat{IQ}_t}{\hat{IV}_t^2}}} \tag{8}$$

where $\hat{IQ}_t$ is a consistent estimator of the integrated quarticity, $\nu_{\hat{IV}}$ and ν_{RV} are constant such that

$$\mathrm{Var}\left[\hat{IV}_t\right] = \frac{\nu_{\hat{IV}_t}}{M} IQ_t + O\left(M^{-2}\right) \quad \text{and} \quad \mathrm{Var}\left[RV_t\right] = \frac{\nu_{RV_t}}{M} IQ_t$$

therefore $\nu_{RV} = 2$ while $\nu_{\hat{IV}}$ depends on the estimator $\hat{IV}$. The test statistics Z_t converges asymptotically to a standard normal random variable. A jump is detected with the confidence level $1-\alpha$ when $Z_t > \Phi_{1-\alpha}^{-1}$ being $\Phi_{1-\alpha}^{-1}$ the inverse standard normal distribution evaluated at $1-\alpha$. In the original proposal of BNS, $\hat{IV}_t$ coincides with BPV_t and $\hat{IQ}_t = \max(\hat{IV}_t^2, QP_t)$ being QP_t the quad-power quarticity. The large diffusion of this test statistics is due to its suitable finite sample properties highlighted by Huang and Tauchen (2005).

An interesting alternative volatility measure is the corrected threshold bipower variation of Corsi, Pirino, and Renò (2010):

$$C-TBPV_t \equiv \mu_1^{-2} \sum_{i=2}^{M} Z_1\left(r_{t,i-1}, c_\theta^2 \hat{v}_{t,i-1}; c_\theta\right) Z_1\left(r_{t,i}, c_\theta^2 \hat{v}_{t,i}; c_\theta\right) \tag{9}$$

where

$$Z_\gamma\left(x, y; c_\theta\right) \equiv \begin{cases} |x|^\gamma & \text{if } x^2 \le y \\ \dfrac{1}{2\Phi\left(-c_\theta\right)\sqrt{\pi}} \left(\dfrac{2}{c_\theta^2} y\right)^{\gamma/2} \Gamma\left(\dfrac{\gamma+1}{2}, \dfrac{c_\theta^2}{2}\right) & \text{if } x^2 > y \end{cases}$$

Φ is the cumulative standard normal distribution and $\Gamma(\alpha, x)$ is the upper incomplete gamma function. The $C-TBPV_t$ replaces the absolute returns exceeding the threshold by their conditional expected value under the normality assumption:

$$\mathbb{E}\left[\left|r_{t,i}\right|^\gamma \middle| \, r_{t,i}^2 > c_\theta^2\right] = Z_\gamma\left(r_{t,i}, c_\theta^2 \hat{v}_{t,i}; c_\theta\right)$$

The corrected threshold tripower quarticity is analogously defined as:

$$C-TTPV_t \equiv \mu_1^{-2} \sum_{i=3}^{M} Z_{4/3}\left(r_{t,i-2}, c_\theta^2 \hat{v}_{t,i-2}; c_\theta\right) Z_{4/3}\left(r_{t,i-1}, c_\theta^2 \hat{v}_{t,i-1}; c_\theta\right) Z_{4/3}\left(r_{t,i}, c_\theta^2 \hat{v}_{t,i}; c_\theta\right) \tag{10}$$

Asymptotically, the $C-TBPV_t$ and the $C-TTPV_t$ behave analogously to the bipower variation and the tripower quarticity in absence of jumps, provided that the threshold vanishes more slowly than the modulus of continuity of the Brownian motion. In presence of jumps instead the upward bias which usually affects the multipower variation measures of Barndorff-Nielsen, Shephard, and Winkel (2006) is drastically reduced, with positive effects on the power of the test. The simulation study of Corsi, Pirino, and Renò (2010) shows that the gain is particularly relevant in presence of consecutive jumps when the bias affecting the multipower variations

can become extremely large with detrimental effects on jump detection. In view of that, we follow the methodology of Corsi, Pirino, and Renò (2010) within the BNS family and as a proxy for the instantaneous volatility we adopt the estimator defined by Equation (14) in the next paragraph. Remarkably, while the LM type of tests described below require substantial restriction to the volatility process, those belonging to the BNS family are more robust and they remain consistent even in presence of volatility jumps, although their power and their size in finite samples can be affected by violent volatility shocks.

3.1.1.1. Identification of intraday jump times. All the tests belonging to the BNS family are designed to reveal the presence of at least one jump over a certain time period, typically a single trading day. In this study, we follow the procedure described in Andersen et al. (2010) based on the iterative application of the BNS test removing at each step the contribution of the largest absolute return from the realized variance. However, we adopt this method with some important modifications:

(1) In the BNS test we use the threshold bipower variation of Corsi, Pirino, and Renò (2010) to reduce the bias due to jumps.
(2) The test is calculated after rescaling high-frequency returns to remove the intraday periodicity of volatility as recommended by Rognlie (2010). This procedure reduces the bias in the bipower variation generated by time varying volatility.
(3) To reduce the bias due to stale quotes documented by Kolokolov and Renò (2018), we remove null intraday returns from the sample before computing the realized measures.
(4) Following Gilder, Shackleton, and Taylor (2014) we classify as a jump the largest absolute log return after adjusting for the intraday volatility pattern.
(5) Differently from Andersen et al. (2010), we recalculate at each step the threshold bipower variation and the tripower quarticity to guarantee the removal of the upward bias in case of jumps.
(6) To limit the effects on the size of the test due to multiple hypotheses testing, we apply the conservative Holm-Bonferroni correction.

3.1.2. The LM family of tests

The LM test is based on a measurement of the instantaneous volatility σ_t. Such a measurement is feasible with asymptotically infinite precision only if the drift μ_t and σ_t itself change 'slowly' in time (see Lee and Mykland 2008 for further details). Such a restriction is the major limitation for these tests since their consistency is not guaranteed in the presence of volatility jumps. The tests statistics within this family is generally defined as follows:

$$z_{t,i} = \frac{|r_{t,i}|}{\sqrt{\hat{V}_{t,i}}} \tag{11}$$

where $\hat{V}_{t,i}$ is an estimator of the instantaneous volatility and $z_{t,i}$ is the normalized absolute return. As the sampling frequency increases, $\hat{V}_{t,i}$ converges to the unobserved instantaneous volatility and $z_{t,i}$ distributes as the absolute value of a standard normal random variable. A jump is detected whenever $z_{t,i}$ exceeds a predetermined threshold θ. The various LM tests proposed in the literature differ for the methodology used to determine the threshold level and for the estimation of the instantaneous volatility. Concerning the threshold, as the test is applied for every intraday return, the issue of false discovery rate (FDR) arising in the context of multiple hypotheses testing must be properly taken into account. The simplest solution (proposed by Andersen, Bollerslev, and Diebold 2007b) consists in the application of the Šidák approach: given a certain daily size α, the corresponding size for each intraday test is $\beta = 1 - (1 - \alpha)^{1/M}$ and the associated threshold level is $\theta = \Phi^{-1}_{1-\beta/2}$. However, finite sample volatility is always measured with an error and the Šidák approach often leads to over-reject the null. LM propose to calculate critical values from the limiting distribution of the maximum of the test statistics: as $M \to \infty$ the quantity

$$\xi_M = \frac{\max_i \left(z_{t,i}\right) - C_M}{S_M}$$

with $C_M = (2\log M)^{1/2} - [\log 4\pi + \log(\log M)]/2\sqrt{2\log M}$ and $S_M = (2\log M)^{-1/2}$, distributes as a Gumbel random variable.[2] This method is more conservative and reduces the probability of detecting spurious jumps.

With regard to the estimators used for the instantaneous volatility, LM propose the bipower variation calculated over a time window of size K depending on the sampling frequency.[3] Andersen, Bollerslev, and Diebold (2007b) use instead the bipower variation calculated over the entire trading day. It is important to remark that both of them are upward biased in case of jumps and may substantially lose accuracy when the instantaneous volatility moves rapidly. These issues are extremely relevant for our purposes: the former reduces the detection power of the test, especially when multiple jumps occur closely in time, and it may also influences the observed clustering pattern; the latter increases the error affecting our local volatility estimates and therefore the probability of spurious jump detection.

To remove the bias, Bormetti et al. (2015) construct an estimator similar to LM which is based on the threshold bipower variation: the past information is weighted through an exponential moving average. The estimator also takes into account the U-shaped intraday volatility pattern that is largely documented in the literature (see for instance Bollerslev, Todorov, and Li 2013; Gilder, Shackleton, and Taylor 2014). In details, let $\tilde{r}_{t,i}$ denote the log-return scaled by a proper factor to remove the intraday periodicity: $\tilde{r}_{t,i} = r_{i,t}/\zeta_i$. The local volatility estimator is defined as

$$\tilde{V}_i^{BEW} = \frac{\alpha}{\mu_1^2}\left|\tilde{r}_{j'}\right|\left|\tilde{r}_j\right| + (1-\alpha)\ \tilde{V}_{i-1}^{BEW} \quad i = 1,\ldots,M\cdot T \tag{12}$$

$$\hat{V}_{t,k}^{BEW} = \zeta_k\ \tilde{V}_{t,k}^{BEW} \quad t = 1,\ldots,T\ k = 1,\ldots,M \tag{13}$$

where $\tilde{V}$ indicates the estimated volatility purified by the intraday volatility pattern[4] ζ_i, $j < j' \leq i-1$, $|\tilde{r}_j|/\sqrt{\hat{V}_j^{BEW}} \leq \theta$ and $|\tilde{r}_l|/\sqrt{\hat{V}_l^{BEW}} > \theta\ \forall\ j < l < j'$. This estimator is a moving average weighted bipower variation excluding all the observation that exceed the threshold θ. However, the inaccuracy in presence of fast volatility changes still remains a critical issue to deal with. We address the problem as follows: (i) to correct the intraday volatility patterns we follow the method proposed by Boudt, Croux, and Laurent (2011) which ensures accuracy and consistency in presence of jumps; (ii) to improve the accuracy in presence of sharp volatility changes, we also consider the estimator $\hat{V}^{FEW}$ based on forward information and defined exactly as $\hat{V}^{BEW}$ but on the time reversed series (i.e. the series obtained substituting the index i with $M\cdot T - i + 1$). Our new estimator is

$$\hat{V}_i^{SEW} = \frac{1}{2}\left(\hat{V}_i^{BEW} + \hat{V}_i^{FEW}\right) \tag{14}$$

which is symmetric in time, i.e. it equally weighs past and future information. With an increasing literature pointing towards the occurrence of volatility jumps (Jacod and Todorov 2010; Todorov and Tauchen 2011; Corsi and Renò 2012; Wei 2012; Christensen, Oomen, and Podolskij 2014; Bandi and Renò 2016), the combination of backward and forward information supports the effectiveness of our jump identification methods. To figure out this point, consider that in presence of an upward volatility jump, the backward estimator tends to underestimate volatility and it is likely to signal spurious price jumps. A simulation study available upon request shows that this approach has remarkably more power compared to the original specification proposed by LM.

3.2. Results

Table 1 reports the summary statistics for the three alternative sets of jumps: the first set obtained from our modified version of the LM test (m-LM henceforth), the second set from sequential version of the CPR test (s-CPR), while the third set comes as the intersection of the previous two. The content of this table can be linked to Figures 2 and 3 which display the time series of jumps identified by the three detection methods. From Table 1, we note significant differences between the outcomes of m-LM and the s-CPR methods: the m-LM test always detects more jumps (almost twice of those detected under the s-CPR test). According to our simulation analysis, we also find that the LM-type of tests have generally more power than the BNS test confirming the results of Dumitru and Urga (2011) and Gilder, Shackleton, and Taylor (2014).

Table 1. Jumps detection – empirical estimates.

	S&P 500			ESTX 50		
	m-LM	s-CPR	m-LM ∩ s-CPR	m-LM	s-CPR	m-LM ∩ s-CPR
days with jumps	235	167	105	465	282	222
total jumps	314	196	118	629	351	255
max. jumps per day	6	5	3	5	7	3
contrib. price var.	3.70%	2.35%	1.75%	6.55%	4.03%	3.46%
average jump size	0.44%	0.40%	0.48%	0.50%	0.52%	0.59%
max. jump size	3.67%	2.64%	2.64%	3.40%	3.40%	3.40%
min. jump size	0.09%	0.08%	0.13%	0.12%	0.04%	0.12%
FDR	7.6%	14.5%	3.2%	3.9%	9.0%	1.5%

Note: Summary statistics for jumps detected under different methods. The m-LM and the s-CPR tests are applied with a nominal confidence level equal to 99.5% and 99% respectively. The contribution of jumps to the total price variance is calculated as the sample average of the ratio between the sum of squared detected jumps and the realized quadratic variation on each trading day (overnight returns are excluded from the denominator).

We observe that all the jump detection methods benefit significantly from the intraday volatility pattern correction which largely reduces the size in finite samples while the market microstructure noise has minor effects at 5 minutes. Importantly, the identification errors of the m-LM and the s-CPR tests are not independent: the size of the intersection is larger than the product of their individual size. The intersection however ensures a large decrease of the actual size making the detection mechanism much more severe. Bajgrowicz, Scaillet, and Treccani (2016) claim that the role of price jumps in the literature is probably overstated because a large fraction of jumps detected non-parametrically are spurious. To avoid drawing wrong conclusions about the dynamics of jumps they suggest to control the Family Wise Error Rate (FWER) or the FDR. The expected false discovery rates on Table 1 are calculated using the size estimated on our numerical simulation.

The relative contribution of jumps to the total price variance is calculated here as the sample average over all trading days of the ratio between the sum of squared jumps and the realized quadratic variation. Huang and Tauchen (2005) instead consider the sample mean of RJ_t (see Equation (7)) calculated using $\hat{IV}_t = BPV_t$ and they find that about 7.3% of the quadratic variation on the S&P 500 is due to jumps. Performing the same calculation on our data with $\hat{IV} = C - TBPV_t$ yields an average ratio of 8.0% for the S&P 500 and 9.3% for the Euro Stoxx 50. Note that these estimates differ significantly from the results of Table 1. Interestingly, the mean of RJ_t on days where no jumps are detected according to the s-CPR test at the 99% confidence level is respectively 4.5% and 4.6% for the two indexes. These result can be interpreted in two different ways that are not mutually exclusive: (1) our choice of the confidence level is too severe to effectively remove the majority of jumps; (2) even after the corrections we adopted to take into account the intraday volatility pattern, the threshold bipower variation is still seriously downward biased. Christensen, Oomen, and Podolskij (2014) find that the contribution of jumps to total price variance extracted from 5 minutes data is usually overestimated and intraday volatility bursts[5] are often misclassified as jumps. Using data sampled at higher frequencies and applying specific corrections for the microstructure noise, they find that the contribution of jumps is much smaller (around 1% for the equity market), a result also confirmed by Bajgrowicz, Scaillet, and Treccani (2016). We therefore maintain severe confidence levels to avoid excessive spurious detection rates. Moreover, we also notice that under all identification procedures, the number of jumps as well as their size and their relative contribution to total price variance are smaller for the U.S. index compared to the Euro Stoxx 50, which can be plausibly related to the lower diversification of the European index.

Figures 4 and 5 show the intraday distribution of jump times. For the purpose of this study, we only focus on jump intraday periodicity and do not investigate in detail the specific events triggering a jump in the process as we prefer to concentrate on the identification of jumps and on their modelling via Hawkes specifications.[6] The pattern of intraday jumps clearly suggests detected jumps can be somehow related to macroeconomic releases and other scheduled announcements. For the U.S. market we notice a peak at about 30 minutes after the market opening (less pronounced under the s-CPR method) which corresponds to the macroeconomic announcements scheduled around 10 o'clock (see Gilder, Shackleton, and Taylor 2014). A second and more evident peak on the

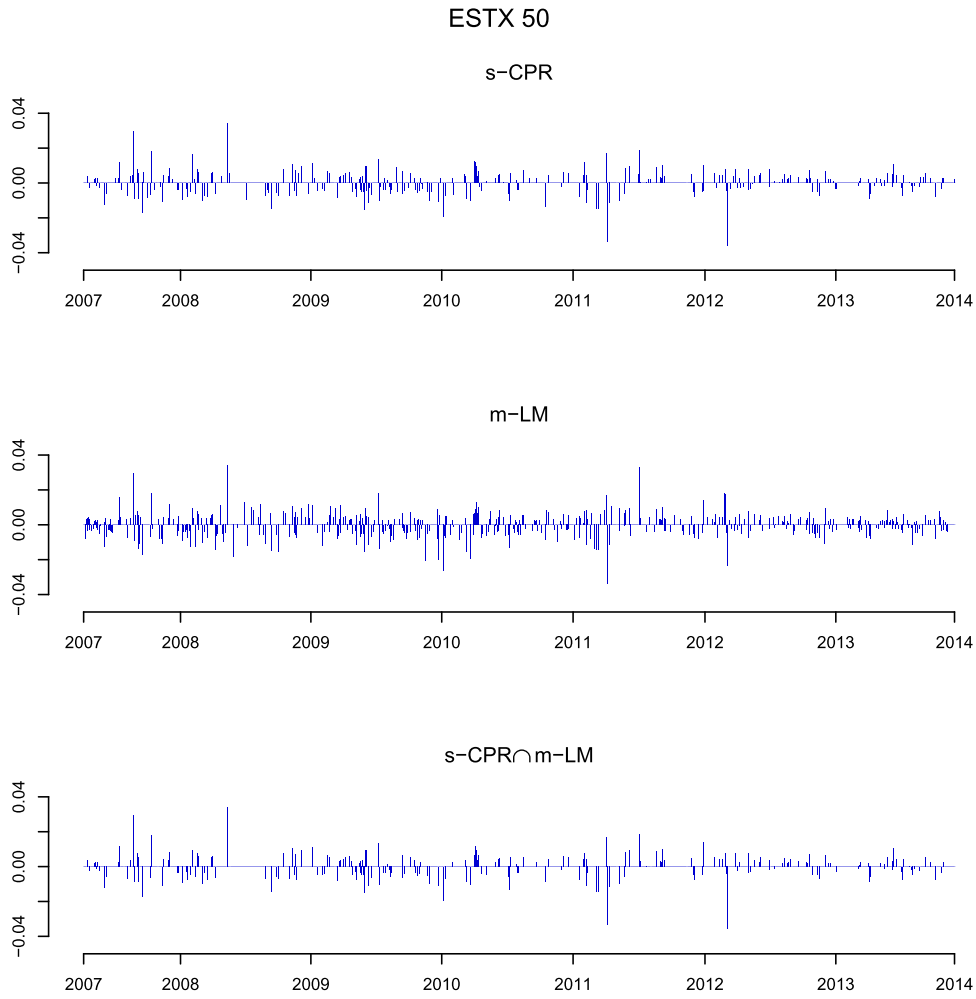

Figure 2. Jumps in the Euro Stoxx 50 identified under different detection methods.

U.S. market is located around 14:00 corresponding to the time at which the Federal Fund Target Rate is publicly communicated after the FOMC meeting. For the European market we observe a large number of jumps located within 14:30 and 14:35 in local time, corresponding to the start of the pre-negotiation at the NYSE. A second and smaller peak is visible 1 hour and a half later, in correspondence of the U.S. macroeconomic announcements previously mentioned, suggesting some cross market dependences of the jump activity in the European market due to news on the U.S. economy.

Figures 6 and 7 report the intraday annualized volatility measured by the square root of the quadratic variation (also including the contribution of jumps). The average number of jumps and the average relative contribution of jumps to the quadratic variation are also reported. All figures show that jumps occur more frequently during low volatility periods. Remarkably, also the relative contribution of jumps is larger when the volatility is lower, regardless of the identification method. This result differentiates us from the findings obtained using daily data and a parametric model by ADL who report that price jumps are more frequent during periods of market turmoil. A possible explanation for this discrepancy is the different time scale of our observations, as the use of high-frequency data allows to disentangle jumps from continuous returns more effectively; in principle this should reduce the risk of misinterpreting a volatility spillover with a jump propagation across markets. In this respect, note that the inverse relation between the volatility level and the relative contribution of jumps is even

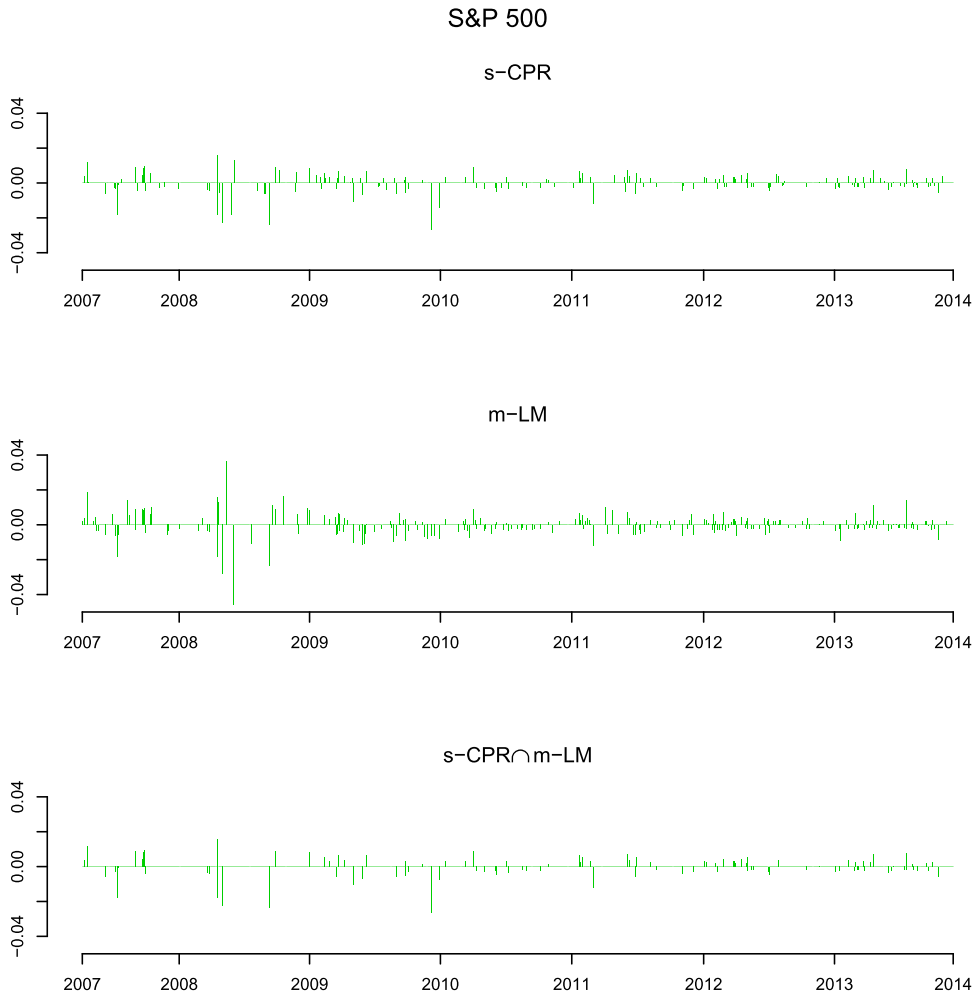

Figure 3. Jumps in the S&P 500 identified under different detection methods.

more pronounced when the continuous volatility is measured by the threshold bipower variation or using the $MinRV_t$ and the $MedRV_t$ measures proposed by Andersen, Dobrev, and Schaumburg (2012). This evidence is quite strong since in the presence of large volatility shocks the bipower variation is downward biased leading to underestimation of the relative contribution of jumps. Thus the effects reported on Figures 6 and 7 cannot be induced by this finite sample bias, with our empirical evidence pointing to a minor role of jumps throughout the subprime and the Euro Sovereign crisis.

4. Modelling jumps with multivariate Hawkes processes

Hawkes processes belong to the class of multivariate point processes characterized by the presence of a conditional intensity vector. They have been originally introduced by Hawkes (1971a, 1971b) and widely used in many different fields including seismology, neuroscience, finance and insurance. The use of Hawkes processes in finance has been pioneered among others by Bowsher (2007) to describe security market transactions and, since then, these models have become increasingly popular in the financial econometrics literature. Thanks to their flexible functional specification, Hawkes processes can be successfully adopted to model the intraday market dynamics using high-frequency data. The conditional intensity of the process can be enriched with selected

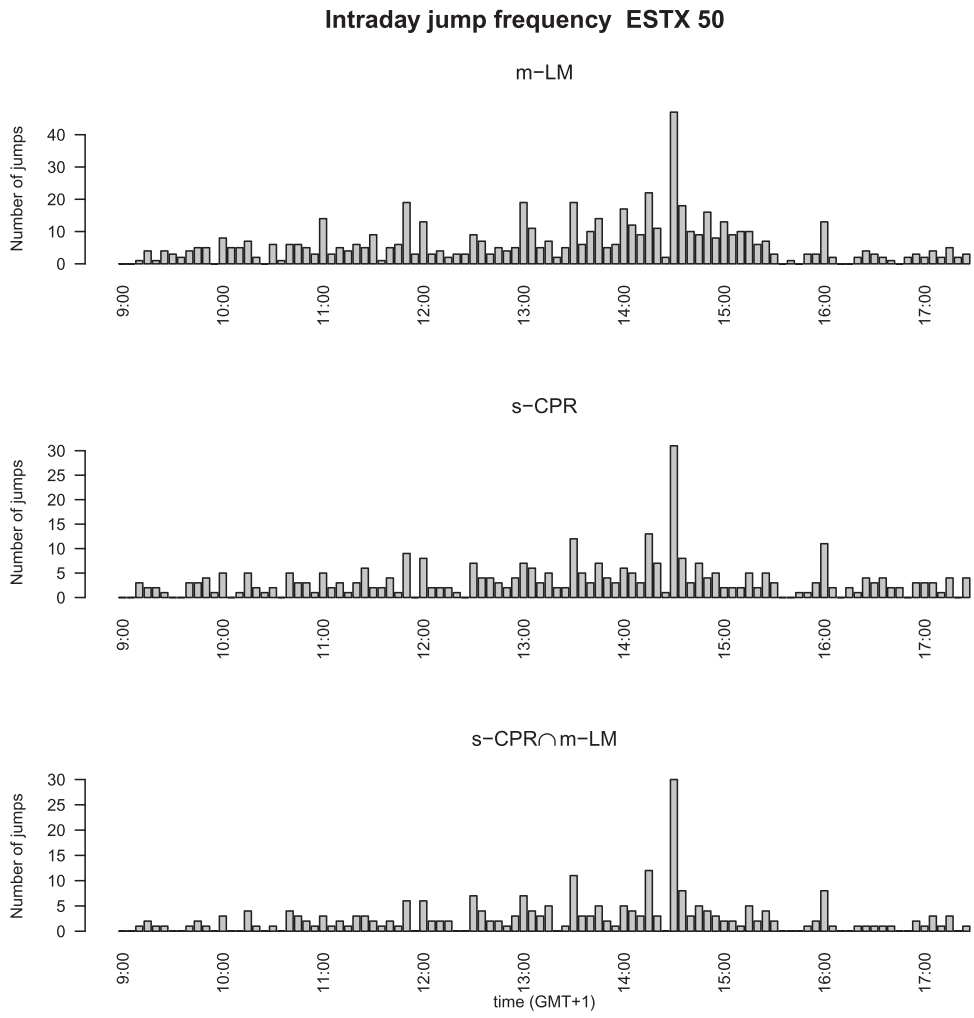

Figure 4. Distribution of intraday jump times for the Euro Stoxx 50.

covariates (or marks) which makes the Hawkes specification particularly suited to describe and test several market microstructure hypotheses including the interaction between different types of market events. Moreover the analytical tractability of Hawkes processes under mild regularity conditions facilitate their estimation and statistical inference (see Bacry, Mastromatteo, and Muzy 2015 for an overview of Hawkes applications in finance). Without claiming to be exhaustive, besides Bowsher (2007) some relevant studies applying Hawkes specifications also include ADL who model contagion through jump cascades involving multiple markets, Embrechts, Liniger, and Lin (2011) present a multivariate Hawkes process with dependent marks modeled through a Gauss copula, Chavez-Demoulin and McGill (2012) adopt the Hawkes process to estimate quantile based measures of risk for intraday financial data, Bormetti et al. (2015) analyze the multivariate dynamics of jumps in the Italian stock market, Granelli and Veraart (2016) examine the variance risk premium on an index whose constituents are subject to contagion, and Clements and Liao (2017) model jumps and co-jumps in the DJIA index and its components. We refer to Hawkes (2018) for a comprehensive review of the most recent contributions in this field.

In this study, we use the Hawkes processes to describe the evolution of the jump intensities $\lambda_{l,\tau}$ where l takes the value 1 for the Euro Stoxx 50 index and 2 for the S&P 500. We will use the notation $\tau(t, i)$ to denote the time

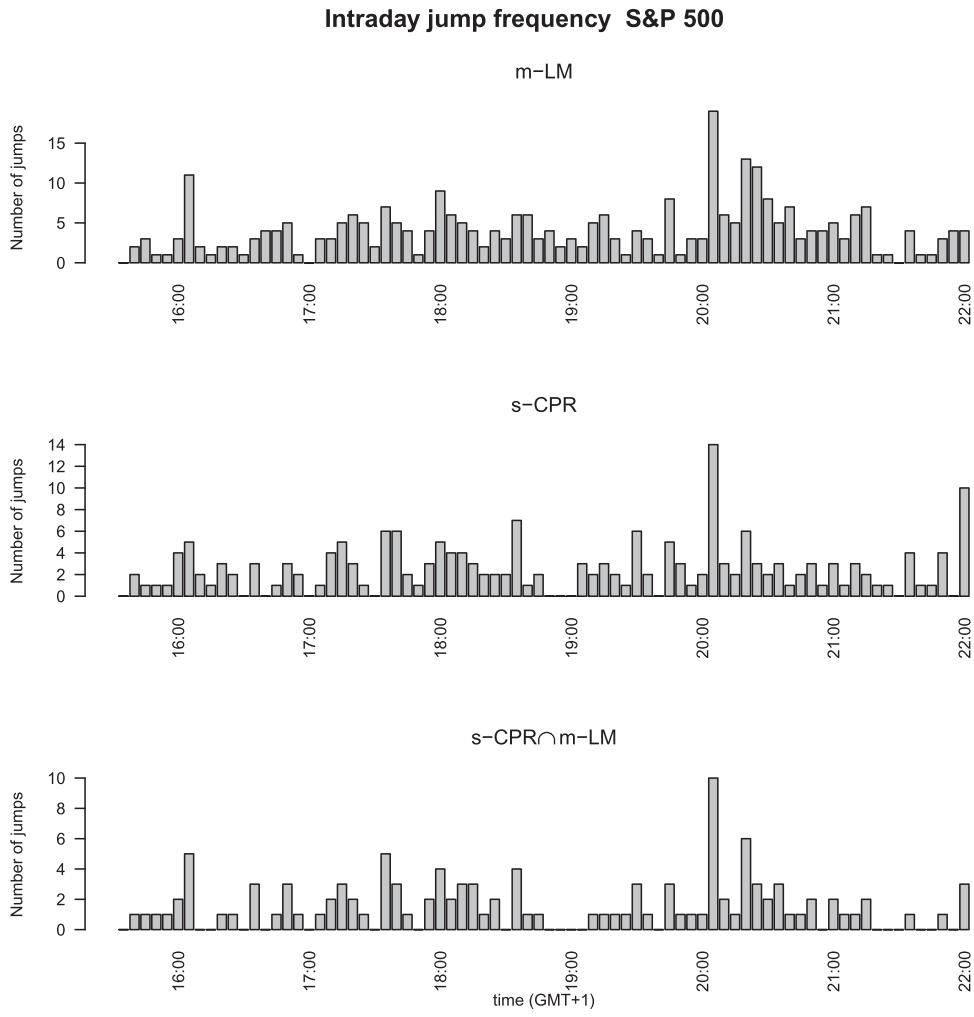

Figure 5. Distribution of intraday jump times for the S&P 500.

corresponding to the ith interval on day t. The standard specification for the jumps intensities is

$$\lambda_{l,\tau} = \theta_l + \sum_{l'=1}^{2} \int_{-\infty}^{\tau} g_{l,l'}(\tau - s)\, \mathrm{d}N_{l',s} \quad l = 1, 2 \tag{15}$$

where θ_l represents the baseline deterministic component, $N_{l,\tau}$ is the counting process for market l and the function $g_{l,l'}$ (usually a negative exponential), measures the effect that an event on market l' generates on the intensity of market l. This model is able to produce jump clustering, because jumps affect the future intensity whenever $g_{l,l} > 0$, as well as cross-excitation effects from l' to l when $g_{l,l'} > 0$ for $l \neq l'$. We use some simple variants of this model to describe the dynamics of jumps detected from high-frequency data: our applications require to take into account that the NYSE and the FSX operate at different times with modest overlaps of the trading activity (normally 2 hours). Moreover trading and non-trading days can differ across countries due to specific national holidays. When the market is closed the jump intensity must be zero, nevertheless the information coming from other operating markets could affect the jump intensity on the next trading day. Equation (15) is appropriate to describe each market during its operating time and when the market l' is closed we can have

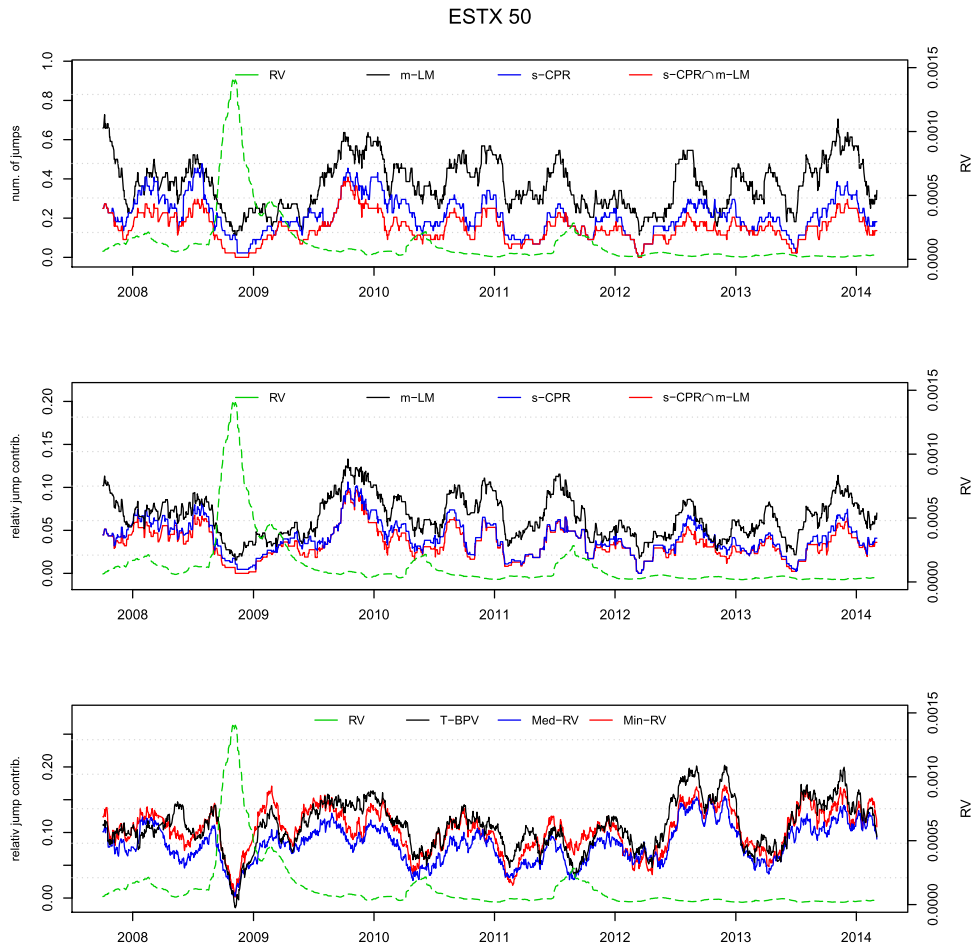

Figure 6. The top panel reports the average number of jumps, the central and the bottom panels show the average contribution of jumps to total price variance calculated respectively from detected jumps and from jump robust realized measures. The dashed line is the intraday realized volatility. All these quantities are averaged over a rolling window of two months centered on the reference date.

only self-excitation effects in market l given that no jumps can occur on l'. The missing part of the dynamics is the overnight evolution of λ_l which obviously requires some specific assumptions. Let $o_{l,t}$ and $c_{l,t}$ denote the opening and closing time of market l measured according to some time convention (for instance UTC); in non-trading days the opening and the closing time coincide: $o_{l,t} = c_{l,t}$. We consider the following recursive evolution:

$$\lambda_{l,\tau} = \begin{cases} \theta_l + \sum_{l'=1}^{2} K_{l,l'} \int_{-\infty}^{\tau} \mathrm{e}^{-\gamma_{l,l'}(\tau-s)} \mathrm{d}N_{l',s} & \tau \in [o_{l,t}, c_{l,t}) \\ 0 & \tau \in [c_{l,t}, o_{l,t+1}) \end{cases} \tag{16}$$

where γ controls the speed of mean reversion while $K_{l,l'}$ establishes the size of self and mutual excitations. In principle different coefficients could be introduced for intraday and overnight periods at the cost of making the equations more complicated but according to our analysis[7] the improvement of the fit is negligible.

Table 2 reports the maximum likelihood estimates of our model enriching the dynamics progressively. Model 1 is a simple Poisson process with constant intensity, obtained imposing $K_{l,l'} = 0$ for $l, l' = 1, 2$. Model 2

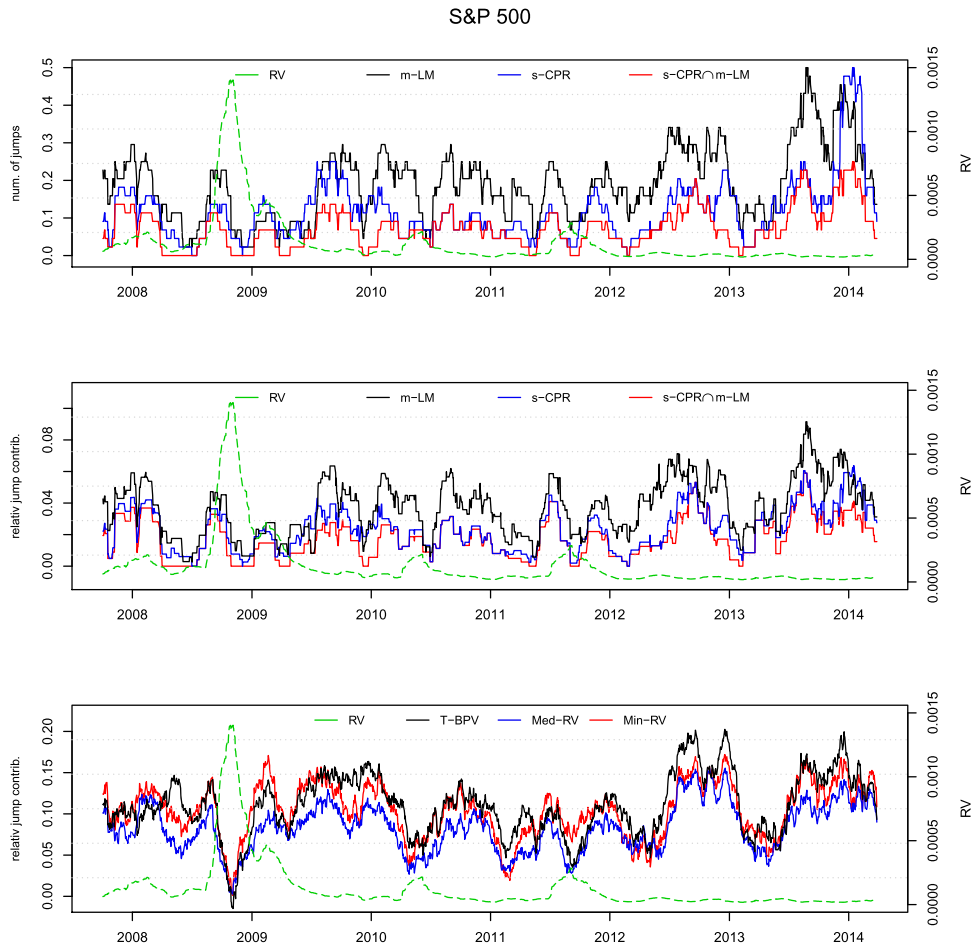

Figure 7. The top panel reports the average number of jumps, the central and the bottom panels show the average contribution of jumps to total price variance calculated respectively from detected jumps and from jump robust realized measures. The dashed line is the intraday realized volatility. All these quantities are averaged over a rolling window of two months centered on the reference date.

is a univariate Hawkes process that includes self-excitation: the restrictions are $K_{l,l'} = 0$ for $l \neq l'$. The effect of jumps on future intensity exhibits a very short persistence: for the S&P 500 the half-life time ranges from 21 min to 1 hour, for the ESTX from 20 min to 1 hour and half. For both markets the jump intensity is more persistent under the s-CPR method. When allowing for self-excitation, we obtain a remarkable increase of the likelihood under all jump identification methods suggesting that jump clustering is an important feature of the jump dynamics. When a jump occurs, its impact on the intensity is remarkably large, generally one order of magnitude larger then the baseline intensity level θ. These results are very similar to those obtained by Bormetti et al. (2015) analyzing the Italian stock market.

Model 3 also includes spillovers in the jump activity (cross-excitation). According to our results cross-excitations are generally insignificant (Table 2).

To extend our analysis, we also explore some additional features of the jump process: the dependence from continuous volatility and the role of the jump size. To this purpose we move from the standard Hawkes processes to the class of generalized Hawkes processes whose properties are discussed in details by Bowsher (2007): the generalized specification allows the deterministic component θ to be time dependent and the impact of jumps

Table 2. MLE for standard Hawkes process.

		ESTX			S&P 500		
		m-LM	s-CPR	Intersection	m-LM	s-CPR	Intersection
model 1	θ	$7.44 \cdot 10^{-4***}$	$4.16 \cdot 10^{-4***}$	$3.02 \cdot 10^{-4***}$	$4.89 \cdot 10^{-4***}$	$3.05 \cdot 10^{-4***}$	$1.84 \cdot 10^{-4***}$
		$(2.56 \cdot 10^{-5})$	$(1.75 \cdot 10^{-5})$	$(1.51 \cdot 10^{-5})$	$(2.23 \cdot 10^{-5})$	$(1.86 \cdot 10^{-5})$	$(1.28 \cdot 10^{-5})$
	log L	−4147.614	−2518.953	−1911.414	−2202.424	−1467.042	−943.060
model 2	θ	$6.32 \cdot 10^{-4***}$	$3.65 \cdot 10^{-4***}$	$2.81 \cdot 10^{-4***}$	$3.95 \cdot 10^{-4***}$	$2.73 \cdot 10^{-4***}$	$1.67 \cdot 10^{-4***}$
		$(2.84 \cdot 10^{-5})$	$(1.88 \cdot 10^{-5})$	$(1.57 \cdot 10^{-5})$	$(2.47 \cdot 10^{-5})$	$(1.97 \cdot 10^{-5})$	$(1.33 \cdot 10^{-5})$
	γ	$3.05 \cdot 10^{-2***}$	$7.45 \cdot 10^{-3**}$	$3.25 \cdot 10^{-2**}$	$2.90 \cdot 10^{-2***}$	$1.15 \cdot 10^{-2**}$	$3.29 \cdot 10^{-2**}$
		$(6.08 \cdot 10^{-3})$	$(2.99 \cdot 10^{-3})$	$(1.52 \cdot 10^{-2})$	$(6.37 \cdot 10^{-3})$	$(5.08 \cdot 10^{-3})$	$(1.41 \cdot 10^{-2})$
	$K_{l,l}$	$4.69 \cdot 10^{-3***}$	$1.20 \cdot 10^{-3***}$	$2.27 \cdot 10^{-3**}$	$5.95 \cdot 10^{-3***}$	$1.57 \cdot 10^{-3***}$	$3.09 \cdot 10^{-3**}$
		$(9.33 \cdot 10^{-4})$	$(3.39 \cdot 10^{-4})$	$(1.04 \cdot 10^{-3})$	$(1.32 \cdot 10^{-3})$	$(5.75 \cdot 10^{-4})$	$(1.47 \cdot 10^{-3})$
	log L	−4062.034	−2489.863	−1895.516	−2116.161	−1448.232	−927.291
model 3	θ	$5.83 \cdot 10^{-4***}$	$2.56 \cdot 10^{-4***}$	$2.70 \cdot 10^{-4***}$	$3.75 \cdot 10^{-4***}$	$2.06 \cdot 10^{-4***}$	$1.62 \cdot 10^{-4***}$
		$(3.59 \cdot 10^{-5})$	$(5.03 \cdot 10^{-5})$	$(1.65 \cdot 10^{-5})$	$(2.85 \cdot 10^{-5})$	$(3.62 \cdot 10^{-5})$	$(1.55 \cdot 10^{-5})$
	γ	$3.06 \cdot 10^{-2***}$	$7.07 \cdot 10^{-3**}$	$3.24 \cdot 10^{-2**}$	$2.87 \cdot 10^{-2***}$	$1.19 \cdot 10^{-2**}$	$3.27 \cdot 10^{-2**}$
		$(6.11 \cdot 10^{-3})$	$(2.88 \cdot 10^{-3})$	$(1.51 \cdot 10^{-2})$	$(6.30 \cdot 10^{-3})$	$(5.30 \cdot 10^{-3})$	$(1.40 \cdot 10^{-2})$
	$K_{l,l}$	$4.68 \cdot 10^{-3***}$	$1.18 \cdot 10^{-3***}$	$2.25 \cdot 10^{-3**}$	$5.89 \cdot 10^{-3***}$	$1.56 \cdot 10^{-3***}$	$3.06 \cdot 10^{-3**}$
		$(9.36 \cdot 10^{-4})$	$(3.31 \cdot 10^{-4})$	$(1.03 \cdot 10^{-3})$	$(1.31 \cdot 10^{-3})$	$(5.81 \cdot 10^{-4})$	$(1.45 \cdot 10^{-3})$
	$\gamma_{l,l'}$	$3.89 \cdot 10^{-4}$	$1.08 \cdot 10^{-5}$	$6.05 \cdot 10^{-4}$	$3.76 \cdot 10^{-3}$	$1.21 \cdot 10^{-4}$	$1.25 \cdot 10^{-3}$
		$(2.98 \cdot 10^{-4})$	$(9.51 \cdot 10^{-6})$	$(7.87 \cdot 10^{-4})$	$(5.34 \cdot 10^{-3})$	$(8.03 \cdot 10^{-5})$	$(5.51 \cdot 10^{-3})$
	$K_{l,l'}$	$2.41 \cdot 10^{-4}$	$2.19 \cdot 10^{-5}$	$2.42 \cdot 10^{-4}$	$1.56 \cdot 10^{-4}$	$7.69 \cdot 10^{-5**}$	$4.89 \cdot 10^{-5}$
		$(1.55 \cdot 10^{-4})$	$(1.62 \cdot 10^{-5})$	$(2.92 \cdot 10^{-4})$	$(1.95 \cdot 10^{-4})$	$(3.72 \cdot 10^{-5})$	$(1.15 \cdot 10^{-4})$
	log L	−4057.178	−2486.933	−1893.643	−2114.747	−1444.632	−926.964

Notes: $^{***}p < 0.01$, $^{**}p < 0.05$, $^{*}p < 0.1$.
Estimates for the standard Hawkes process: time is measured in minutes and standard errors are reported in parenthesis.

to depend on the normalized jump size. The full model is specified as follows:

$$\lambda_{l,\tau} = \begin{cases} \theta_{l,\tau} + \sum_{l'=1}^{2} K_{l,l'} \int_{-\infty}^{\tau} \mathrm{e}^{-\gamma_{l,l'}(\tau - s)} \left| \frac{J_{l',s}}{\sqrt{v_{l',s}}} \right|^{\alpha} \mathrm{d}N_{l',s} & \tau \in \left[o_{l,t}, c_{l,t}\right) \\ 0 & \tau \in \left[c_{l,t}, o_{l,t+1}\right) \end{cases} \tag{17}$$

where $\alpha \geq 0$. We consider the following parametrization for the deterministic time dependent component $\theta_{l,\tau}$ used to accommodate an explicit dependence on the continuous volatility level:

$$\theta_{l,\tau} = \exp\left(a_l + b_l \log v_{l,\tau}\right) \quad a_l, b_l \in \mathbb{R} \tag{18}$$

where our volatility proxy is

$$v_{l,\tau(t,i)} = IV_t \, \zeta_i^2 / M \tag{19}$$

IV_t is the integrated volatility on day t, ζ_i is the intraday volatility correction factor taking into account the U-shaped volatility pattern, and M is the number of intraday returns. Equation (19) is a proxy for the instantaneous volatility on a specific time interval i on day t. To avoid any endogeneity bias in the measurement of integrated volatility, we use a forecast of the integrated volatility built on the information available up to day $t-1$ and based on a bivariate extension of the HAR-type regressions.[8]

The dependence on the jump size is introduced in our generalized Hawkes model when $\alpha > 0$ and it is determined by the absolute size of the jump normalized by the instantaneous volatility: the idea is that the impact of a jump is proportional to its size compared to the typical size of continuous returns on the same period. The results for the alternative specifications are reported in Table 3 where the distinctive features of the generalized process are gradually introduced. Model 4 extends the univariate Model 2 and also introduces the volatility dependence under the constraints $\alpha = 0$, $K_{l,l'} = 0$. Importantly, Table 3 shows that all estimates confirm a significant inverse dependence on the volatility level, a result consistent with Wei (2012) who finds that the volatility is on average lower on trading days with jumps. This result confirms what we qualitatively observe

Table 3. MLE for generalized Hawkes process.

		ESTX			S&P 500		
		m-LM	s-CPR	Intersection	m-LM	s-CPR	Intersection
model 4	a	$-1.25 \cdot 10^{1***}$	$-1.13 \cdot 10^{1***}$	$-1.23 \cdot 10^{1***}$	$-1.24 \cdot 10^{1***}$	$-1.08 \cdot 10^{1***}$	$-1.34 \cdot 10^{1***}$
		$(7.88 \cdot 10^{-1})$	$(9.83 \cdot 10^{-1})$	$(9.42 \cdot 10^{-1})$	$(9.81 \cdot 10^{-1})$	(1.01)	(1.34)
	b	$-3.64 \cdot 10^{-1***}$	$-2.44 \cdot 10^{-1***}$	$-2.91 \cdot 10^{-1***}$	$-3.13 \cdot 10^{-1***}$	$-1.82 \cdot 10^{-1***}$	$-3.28 \cdot 10^{-1***}$
		$(5.53 \cdot 10^{-2})$	$(6.94 \cdot 10^{-2})$	$(6.69 \cdot 10^{-2})$	$(6.74 \cdot 10^{-2})$	$(6.90 \cdot 10^{-2})$	$(9.17 \cdot 10^{-2})$
	γ	$3.21 \cdot 10^{-2***}$	$5.72 \cdot 10^{-3**}$	$3.34 \cdot 10^{-2**}$	$3.07 \cdot 10^{-2***}$	$1.22 \cdot 10^{-2**}$	$3.59 \cdot 10^{-2**}$
		$(6.70 \cdot 10^{-3})$	$(2.61 \cdot 10^{-3})$	$(1.66 \cdot 10^{-2})$	$(7.05 \cdot 10^{-3})$	$(5.46 \cdot 10^{-3})$	$(1.65 \cdot 10^{-2})$
	$K_{l,l}$	$4.63 \cdot 10^{-3***}$	$1.05 \cdot 10^{-3***}$	$2.21 \cdot 10^{-3**}$	$6.09 \cdot 10^{-3***}$	$1.57 \cdot 10^{-3***}$	$3.22 \cdot 10^{-3**}$
		$(9.67 \cdot 10^{-4})$	$(3.03 \cdot 10^{-4})$	$(1.08 \cdot 10^{-3})$	$(1.40 \cdot 10^{-3})$	$(5.87 \cdot 10^{-4})$	$(1.60 \cdot 10^{-3})$
	log L	−4036.82	−2483.30	−1888.11	−2103.84	−1445.14	−921.58
model 5	a	$-1.24 \cdot 10^{1***}$	$-1.18 \cdot 10^{1***}$	$-1.23 \cdot 10^{1***}$	$-1.23 \cdot 10^{1***}$	$-1.08 \cdot 10^{1***}$	$-1.35 \cdot 10^{1***}$
		$(7.85 \cdot 10^{-1})$	(1.00)	$(9.41 \cdot 10^{-1})$	$(9.79 \cdot 10^{-1})$	(1.01)	(1.34)
	b	$-3.59 \cdot 10^{-1***}$	$-2.78 \cdot 10^{-1***}$	$-2.91 \cdot 10^{-1***}$	$-3.11 \cdot 10^{-1***}$	$-1.84 \cdot 10^{-1***}$	$-3.30 \cdot 10^{-1***}$
		$(5.51 \cdot 10^{-2})$	$(7.05 \cdot 10^{-2})$	$(6.68 \cdot 10^{-2})$	$(6.72 \cdot 10^{-2})$	$(6.90 \cdot 10^{-2})$	$(9.18 \cdot 10^{-2})$
	γ	$3.21 \cdot 10^{-2***}$	$8.93 \cdot 10^{-3***}$	$3.47 \cdot 10^{-2**}$	$3.01 \cdot 10^{-2***}$	$1.26 \cdot 10^{-2**}$	$4.00 \cdot 10^{-2**}$
		$(6.13 \cdot 10^{-3})$	$(3.26 \cdot 10^{-3})$	$(1.75 \cdot 10^{-2})$	$(6.96 \cdot 10^{-3})$	$(6.09 \cdot 10^{-3})$	$(1.95 \cdot 10^{-2})$
	$K_{l,l}$	$1.78 \cdot 10^{-4}$	$1.43 \cdot 10^{-3}$	$5.66 \cdot 10^{-4}$	$2.97 \cdot 10^{-4}$	$1.02 \cdot 10^{-3}$	$5.52 \cdot 10^{-4}$
		$(1.09 \cdot 10^{-4})$	$(1.10 \cdot 10^{-3})$	$(7.26 \cdot 10^{-4})$	$(1.97 \cdot 10^{-4})$	$(1.05 \cdot 10^{-3})$	$(8.91 \cdot 10^{-4})$
	α	1.81^{***}	–	$7.54 \cdot 10^{-1}$	1.67^{***}	$2.87 \cdot 10^{-1}$	$9.91 \cdot 10^{-1}$
		$(2.92 \cdot 10^{-1})$	–	$(6.13 \cdot 10^{-1})$	$(3.11 \cdot 10^{-1})$	$(5.17 \cdot 10^{-1})$	$(7.03 \cdot 10^{-1})$
	log L	−4019.97	−2483.78	−1887.55	−2089.54	−1445.02	−920.50

Notes: $^{***}p < 0.01$, $^{**}p < 0.05$, $^{*}p < 0.1$.

Estimates for the extended univariate Hawkes process: time is measured in minutes and standard errors are reported in parenthesis. Note that for model 5 for under the s-CPR method the constraint $\alpha \geq 0$ is binding.

in Figures 6 and 7: jumps mostly characterize tranquil market conditions rather than periods of turmoil. The inverse dependence that we measure could also reflect the difficulty of our non-parametric tests to detect jumps when the volatility is high. This may be the case for instance if jumps are i.i.d.: in presence of high volatility levels, the magnitude of continuous price fluctuations observed at a fixed sampling frequency may get close to the magnitude of jumps. The detection of discontinuities would then require a finer time resolution which is usually not achievable in practice due to the presence of the microstructure noise. Besides this statistical-based motivation, the inverse relationship between jumps and volatility could also point to the increasing role of market liquidity as a factor to explain the occurrence of price jumps. Recent contributions in the literature emphasize that abrupt variations of market liquidity are likely to trigger jumps even outside turbulent trading periods, see Jiang, Lo, and Verdelhan (2011), Christensen, Oomen, and Podolskij (2014), Christoffersen et al. (2016) among others.

With regard to cross-market effects, according to our estimates that are not reported here for brevity, none of the cross-excitation coefficients is statistically significant, regardless of the method used to detect jumps (also the weak effects observed under the s-CPR method in model 3 in Table 2 disappear). Concerning the role played by the jump size, we see that there is no agreement across the different detection methods: under the m-LM procedure, large jumps seem to have a larger impact on the intensity with a convex response ($\alpha > 1$); this effect disappears under the s-CPR method and for the intersection set. A possible motivation for this difference would be the presence of volatility jumps: contrary to the s-CPR method that is asymptotically robust to these events, the m-LM method is subject to an increase of the false detection rate. A quick rise in volatility may be erroneously identified as a jump under the m-LM method which may lead to the kind of result that we have observed.

5. Conclusions

We study the statistical properties of the bivariate jump process in the Euro Stoxx 50 and the S&P 500 index, representing two leading stock markets. To the best of our knowledge, this is the first paper studying jump transmission across these markets based on high-frequency data. Our jump identification strategy builds on alternative non-parametric techniques. We find that jumps often occur when macroeconomics announcements

are released and they are more likely to be detected when the continuous volatility is low. In principle, the observed inverse dependence between jump intensity and continuous volatility can also emerge from an identification problem: when the volatility is high it is more difficult to distinguish jumps from continuous returns. However, our results seem to exclude the possibility that jumps played prominent role during the subprime and the Euro Sovereign crisis in 2008–2009 and 2011–2012, respectively. In fact, these periods are characterized by high volatility peaks which overwhelm the jump component in terms of relative contribution to the total price variance. Interestingly, this result adds novel evidence to the literature as it appears in contrast with the findings of ADL, a discrepancy that in our view is likely determined by the different time scale and by the specific parametric assumptions of ADL. In fact, days with large absolute returns are not necessarily characterized by an intense jump activity at a high frequency. We make use of the results from the jump identification stage to model the evolution of the jump intensities via Hawkes processes which are found to be overwhelmingly preferred to a constant intensity Poisson process. The Hawkes specification proves to be successful in capturing jump clustering effects whose time persistence is generally short and therefore unable to produce measurable effects across different trading days. On the other hand, as to contagion effect across markets, our estimates exclude the presence of significant spillovers in the jump activity, a result complementary to the evidence in Corradi, Distaso, and Fernandes (2012) who document significant spillovers across markets affecting the continuous volatility and the absence of cross-market effects triggered by jumps.

Our analysis reveals important features characterizing jump events with relevant implications for asset price modeling, derivatives pricing, risk management, and asset allocation. As an example, if large price fluctuations during periods of stress are mostly determined by continuous volatility, then hedging this risk becomes easier compared to a full insurance against risk emerging either from jump occurrence or even from jump contagion across markets. This is also extremely relevant for option pricing, since the price of short maturity options is strongly affected by jumps. In general, our results indicate that the role of jumps has been probably overstated in the past literature, as it has also been recognized in some recent papers on the topic (Bajgrowicz, Scaillet, and Treccani 2016; Christensen, Oomen, and Renò 2016). Importantly, our evidence also provides several directions for future research. In view of the aforementioned inverse relation between jump intensity and volatility, a first extension would be a more thorough investigation of the relative importance of volatility shocks compared to price jumps in the period 2007–2014. At the intraday level, the analysis of how different types of information releases can generate different outcomes in terms of jump size and clustering may also deserve further investigation.

Notes

1. A simulation study available in the online appendix validates the technical aspects of our methodology.
2. The definition of C_M reports the amended and correct version of the original equation presented in Lee and Mykland (2008). We thank Vincent Tsai for highlighting this point.
3. They recommend $K = \sqrt{252\,M}$ where 252 is the number of trading days in a year.
4. To save space we provide the technical details on the estimation of the intraday correction factor ζ_i in an online Appendix.
5. The recent paper of Christensen, Oomen, and Renò (2016) shows that flash crashes are indeed characterized by drift bursts with a continuous path. Such events cannot be clearly distinguished from jumps at 5 minutes but require a higher frequency to be properly investigated.
6. The analysis of the interplay between jumps and macroeconomic releases would represent a valuable extension of this study though this would also require detailed information on all the relevant news announcements at intraday frequency; we thank an anonymous referee for raising this point and leave this possibility for future research.
7. Estimates are not reported here, but available upon reques.
8. Details on the method applied to estimate the integrated volatility and a general discussion on the volatility spillovers between the two markets are available in the online appendix. of Corsi and Renò (2012).

Acknowledgments

We would like to thank the editor Chris Adcock, two anonymous referees, Monica Billio, Giacomo Bormetti, Fulvio Corsi, Alain Monfort, Sergio Pastorello, Loriana Pelizzon, Roberto Renò, seminar participants at 5th SIdE Workshop and 15th Paris December Finance Meeting for their helpful comments and suggestions. The views expressed in this paper are those of the authors and do not necessarily reflect those of the Bank of Italy or the Eurosystem. All remaining errors are our own.

Disclosure statement

No potential conflict of interest was reported by the author(s).

References

Ait-Sahalia, Y. 2004. "Disentangling Diffusion From Jumps." *Journal of Financial Economics* 74 (3): 487–528.

Ait-Sahalia, Y., and T. R. Hurd. 2015. "Portfolio Choice in Markets with Contagion." *Journal of Financial Econometrics* 14 (1): 1–28.

Aït-Sahalia, Y., J. Cacho-Diaz, and T. R. Hurd. 2009. "Portfolio Choice with Jumps: A Closed-Form Solution." *The Annals of Applied Probability* 19 (2): 556–584.

Aït-Sahalia, Y., J. Cacho-Diaz, and R. J. A. Laeven. 2015. "Modeling Financial Contagion Using Mutually Exciting Jump Processes." *Journal of Financial Economics* 117 (3): 585–606.

Andersen, T. G., L. Benzoni, and J. Lund. 2002. "An Empirical Investigation of Continuous-Time Equity Return Models." *Journal of Finance* 57 (3): 1239–1284.

Andersen, T. G., and T. Bollerslev. 1997. "Intraday Periodicity and Volatility Persistence in Financial Markets." *Journal of Empirical Finance* 4 (2–3): 115–158.

Andersen, T. G., T. Bollerslev, and F. X. Diebold. 2007b. "Roughing it Up: Including Jump Components in the Measurement, Modeling, and Forecasting of Return Volatility." *The Review of Economics and Statistics* 89 (4): 701–720.

Andersen, T. G., T. Bollerslev, and D. Dobrev. 2007a. "No-Arbitrage Semi-Martingale Restrictions for Continuous-time Volatility Models Subject to Leverage Effects, Jumps and I.I.D. Noise: Theory and Testable Distributional Implications." *Journal of Econometrics* 138 (1): 125–180.

Andersen, T. G., T. Bollerslev, P. Frederiksen, and M. Nielsen. 2010. "Continuous-Time Models, Realized Volatilities, and Testable Distributional Implications for Daily Stock Returns." *Journal of Applied Econometrics* 25 (2): 233–261.

Andersen, T. G., D. Dobrev, and E. Schaumburg. 2012. "Jump-Robust Volatility Estimation Using Nearest Neighbor Truncation." *Journal of Econometrics* 169 (1): 75–93.

Bacry, E., I. Mastromatteo, and J. F. Muzy. 2015. "Hawkes Processes in Finance." *Market Microstructure and Liquidity* 1 (1).

Bajgrowicz, P., O. Scaillet, and A. Treccani. 2016. "Jumps in High-Frequency Data: Spurious Detections, Dynamics, and News." *Management Science* 62 (8): 2198–2217.

Bandi, F. M., and R. Renò. 2016. "Price and Volatility Co-Jumps." *Journal of Financial Economics* 119 (1): 107–146.

Barndorff-Nielsen, O. E., and N. Shephard. 2004. "Power and Bipower Variation with Stochastic Volatility and Jumps." *Journal of Financial Econometrics* 2 (1): 1–37.

Barndorff-Nielsen, O. E., and N. Shephard. 2006. "Econometrics of Testing for Jumps in Financial Economics Using Bipower Variation." *Journal of Financial Econometrics* 4 (1): 1–30.

Barndorff-Nielsen, O. E., N. Shephard, and M. Winkel. 2006. "Limit Theorems for Multipower Variation in the Presence of Jumps." *Stochastic Processes and Their Applications* 116 (5): 796–806.

Black, F., and M. S. Scholes. 1973. "The Pricing of Options and Corporate Liabilities." *Journal of Political Economy* 81 (3): 637–654.

Bollerslev, T., T. H. Law, and G. Tauchen. 2008. "Risk, Jumps, and Diversification." *Journal of Econometrics* 144 (1): 234–256.

Bollerslev, T., and V. Todorov. 2011. "Tails, Fears, and Risk Premia." *The Journal of Finance* 66 (6): 2165–2211.

Bollerslev, T., V. Todorov, and S. Z. Li. 2013. "Jump Tails, Extreme Dependencies, and the Distribution of Stock Returns." *Journal of Econometrics* 172 (2): 307–324.

Bormetti, G., L. M. Calcagnile, M. Treccani, F. Corsi, S. Marmi, and F. Lillo. 2015. "Modelling Systemic Price Cojumps with Hawkes Factor Models." *Quantitative Finance* 15 (7): 1137–1156.

Boudt, K., C. Croux, and S. Laurent. 2011. "Robust Estimation of Intraweek Periodicity in Volatility and Jump Detection." *Journal of Empirical Finance* 18 (2): 353–367.

Bowsher, C. G. 2007. "Modelling Security Market Events in Continuous Time: Intensity Based, Multivariate Point Process Models." *Journal of Econometrics* 141 (2): 876–912.

Caporin, M., A. Kolokolov, and R. Renò. 2017. "Systemic Co-Jumps." *Journal of Financial Economics* 126 (3): 563–591.

Chavez-Demoulin, V., and J. A. McGill. 2012. "High-Frequency Financial Data Modeling Using Hawkes Processes." *Journal of Banking & Finance* 36 (12): 3415–3426.

Christensen, K., R. Oomen, and M. Podolskij. 2010. "Realised Quantile-Based Estimation of the Integrated Variance." *Journal of Econometrics* 159 (1): 74–98.

Christensen, K., R. Oomen, and M. Podolskij. 2014. "Fact Or Friction: Jumps at Ultra High Frequency." *Journal of Financial Economics* 114 (3): 576–599.

Christensen, K., R. Oomen, and R. Renò. 2016. "The Drift Burst Hypothesis." Available at SSRN.

Christoffersen, P., B. Feunou, Y. Jeon, and C. Ornthanalai. 2016. "Time-varying Crash Risk: The Role of Market Liquidity." Working paper.

Clements, A., and Y. Liao. 2017. "Forecasting the Variance of Stock Index Returns Using Jumps and Cojumps." *International Journal of Forecasting* 33 (3): 729–742.

Corradi, V., W. Distaso, and M. Fernandes. 2012. "International Market Links and Volatility Transmission." *Journal of Econometrics* 170 (1): 117–141.

Corsi, F. 2009. "A Simple Approximate Long-Memory Model of Realized Volatility." *Journal of Financial Econometrics* 7 (2): 174–196.

Corsi, F., D. Pirino, and R. Renò. 2010. "Threshold Bipower Variation and the Impact of Jumps on Volatility Forecasting." *Journal of Econometrics* 159 (2): 276–288.
Corsi, F., and R. Renò. 2012. "Discrete-Time Volatility Forecasting With Persistent Leverage Effect and the Link With Continuous-Time Volatility Modeling." *Journal of Business & Economic Statistics* 30 (3): 368–380.
Duffie, D., and J. Pan. 2001. "Analytical Value-at-Risk with Jumps and Credit Risk." *Finance and Stochastics* 5 (2): 155–180.
Duffie, D., J. Pan, and K. Singleton. 2000. "Transform Analysis and Asset Pricing for Affine Jump-Diffusions." *Econometrica* 68: 1343–1376.
Dumitru, A. M., and G. Urga. 2011. "Identifying Jumps in Financial Assets: A Comparison Between Nonparametric Jump Tests." *Journal of Business & Economic Statistics* 30 (2): 242–255.
Embrechts, P., T. Liniger, and L. Lin. 2011. "Multivariate Hawkes Processes: An Application to Financial Data." *Journal of Applied Probability* 48 (A): 367–378.
Eraker, B., M. Johannes, and N. Polson. 2003. "The Impact of Jumps in Volatility and Returns." *The Journal of Finance* 58 (3): 1269–1300.
Gilder, D., M. B. Shackleton, and S. J. Taylor. 2014. "Cojumps in Stock Prices: Empirical Evidence." *Journal of Banking & Finance* 40: 443–459.
Granelli, A., and A. Veraart. 2016. "Modelling the Variance Risk Premium of Equity Indices: The Role Ofdependence and Contagion." *SIAM Journal on Financial Mathematics* 7: 382–417.
Hansen, P. R., and A. Lunde. 2006. "Realized Variance and Market Microstructure Noise." *Journal of Business & Economic Statistics* 24: 127–161.
Harris, L. 1986. "A Transaction Data Study of Weekly and Intradaily Patterns in Stock Returns." *Journal of Financial Economics* 16 (1): 99–117.
Hasbrouck, J. 1999. "The Dynamics of Discrete Bid and Ask Quotes." *The Journal of Finance* 54 (6): 2109–2142.
Hawkes, A. G. 1971a. "Point Spectra of Some Mutually Exciting Point Processes." *Journal of the Royal Statistical Society: Series B (Methodological)* 33 (3): 438–443.
Hawkes, A. G. 1971b. "Spectra of Some Self-Exciting and Mutually Exciting Point Processes." *Biometrika* 58 (1): 83–90.
Hawkes, A. G. 2018. "Hawkes Processes and Their Applications to Finance: A Review." *Quantitative Finance* 18 (2): 193–198.
Huang, X., and G. Tauchen. 2005. "The Relative Contribution of Jumps to Total Price Variance." *Journal of Financial Econometrics* 3 (4): 456–499.
Jacod, J., and V. Todorov. 2010. "Do Price and Volatility Jump Together?" *The Annals of Applied Probability* 20 (4): 1425–1469.
Jiang, G. J., I. Lo, and A. Verdelhan. 2011. "Information Shocks, Liquidity Shocks, Jumps, and Price Discovery: Evidence From the U.S. Treasury Market." *Journal of Financial and Quantitative Analysis* 46 (2): 527–551.
Kolokolov, A., and R. Renò. 2017. "Efficient Multipowers." *Journal of Financial Econometrics* 16 (4): 629–659.
Kolokolov, Aleksey, and Roberto Renò. 2018. "Jumps or flatness?" *Working paper.*
Lee, S. S., and P. A. Mykland. 2008. "Jumps in Financial Markets: A New Nonparametric Test and Jump Dynamics." *Review of Financial Studies* 21 (6): 2535–2563.
Liu, J., F. A. Longstaff, and Jun Pan. 2003. "Dynamic Asset Allocation with Event Risk." *The Journal of Finance* 58 (1): 231–259.
Mancini, C. 2009. "Non-parametric Threshold Estimation for Models with Stochastic Diffusion Coefficient and Jumps." *Scandinavian Journal of Statistics* 36 (2): 270–296.
Merton, R. C. 1976. "Option Pricing when Underlying Stock Returns are Discontinuous." *Journal of Financial Economics* 3 (1–2): 125–144.
Rognlie, M. 2010. "Spurious Jump Detection and Intraday Changes in Volatility." Duke University Economics Honor Thesis, Duke University.
Taylor, S. J., and X. Xu. 1997. "The Incremental Volatility Information in One Million Foreign Exchange Quotations." *Journal of Empirical Finance* 4 (4): 317–340.
Todorov, V., and G. Tauchen. 2011. "Volatility Jumps." *Journal of Business & Economic Statistics* 29 (3): 356–371.
Wei, S. 2012. "Simultaneous Occurrence of Price Jumps and Changes in Diffusive price Volatility." Duke University Economics Honor Thesis, Duke University.
Wood, R. A., T. H. McInish, and J. K. Ord. 1985. "An Investigation of Transactions Data for NYSE Stocks." *The Journal of Finance* 40 (3): 723–739.
Wright, J. H., and H. Zhou. 2009. "Bond Risk Premia and Realized Jump Risk." *Journal of Banking & Finance* 33 (12): 2333–2345.

Appendices

Appendix 1. Simulation study

We conducted a Monte Carlo experiment to investigate in details our jump detection and estimation procedures. We simulated 20.000 trading days with a duration of 6 hours and 30 minutes, consistently with the usual operating time of the NYSE. Stochastic volatility is introduced through a log-volatility model with the following dynamics of the continuous log-prices component:

$$\mathrm{d}Y(t) = \mu\,\mathrm{d}t + \sigma_U(t)\,\sqrt{v(t)}\,\mathrm{d}W_1(t) \tag{A1}$$

$$\mathrm{d}\log v(t) = (\beta_0 - \beta_1 v(t))\,\mathrm{d}t + \eta\,\mathrm{d}W_2(t) \tag{A2}$$

where $Y(t)$ is the log-price, W_1 and W_2 are correlated Brownian motions with constant correlation ρ to generate the well known leverage effect. This setting is common to many other simulation experiments including Huang and Tauchen (2005), Corsi, Pirino, and Renò (2010), Dumitru and Urga (2011), Gilder, Shackleton, and Taylor (2014) and Kolokolov and Renò (2017). We set the parameter $\rho = -0.61$ according to the estimates of Andersen, Benzoni, and Lund (2002) and $\mu = 3\%$, while for the evolution of the stochastic volatility we prefer to calibrate the model on our S&P data. To this purpose we estimate the following simple autoregressive model in discrete time

$$\log IV_t = \beta_0 + (1-\beta_1)\log IV_{t-1} + \eta\epsilon_t$$

where IV_t is the continuous realized volatility. From the regression coefficients we find $\beta_0 = -0.0829$, $\beta_1 = 0.128$,$\eta = 0.55$, where time is measured in days and log-returns in percentage. The volatility is unconditionally distributed as a log-normal with location and scale parameters respectively equal to $\beta_0/\beta_1 = -0.648$ and $\eta^2/4\beta_1 = 0.591$, the average daily volatility is $\exp(\beta_0/\beta_1 + \eta^2/4\beta_1) = 0.95\%$ corresponding to an annualized value of 15.52% (assuming 252 trading days per year). Note that the mean reversion is very strong being characterized by a half-life time of 7.8 trading days. The model is clearly unable to capture the long term volatility persistence. However it captures the unconditional mean and variance of the continuous realized volatility. The intraday volatility pattern is introduced following Andersen, Dobrev, and Schaumburg (2012) according to the functional form of Hasbrouck (1999):

$$\sigma_U(t) = C + A\,\mathrm{e}^{-at} + B\,\mathrm{e}^{-b(1-t)} \quad t \in [0,1] \tag{A3}$$

parameters are $A = 0.75$, $B = 0.25$, $B = 0.89$, $a = 10$, $b = 10$. The U-shape associated with this values is very pronounced: the volatility at the opening and at the closing time on each day are respectively 3 and 1.5 times larger than the mid-day volatility. The log-price process is then augmented with i.i.d. normally distributed jumps having zero mean and variance σ_J^2:

$$p_t = Y_t + \int_0^t J_s\,\mathrm{d}N_s$$

where N_t is an independent Poisson counting process having constant intensity $\lambda = 1$ (i.e. on average one jump per day and $\sigma_J = 1\%$). To make our simulation more realistic we also introduce market microstructure noise, assume that prices are observed with an error:

$$\tilde{p}_t = p_t + \epsilon_t \tag{A4}$$

following Gilder, Shackleton, and Taylor (2014), ϵ_t is normal with zero mean and variance equal to 10^{-3} times the daily realized variance to obtain a noise to signal ratio consistent with the empirical findings of Hansen and Lunde (2006). Equations (A1) and (A2) and the jump processes are simulated according to the Euler scheme with a time increment of one second. The simulated data are then sampled at 5 min and each simulated trading day contains therefore 78 log-returns.

Results

The power and the size of each jump detection tests is reported on Table A1. The m-LM test exhibits the largest power and a smaller size compared to s-CPR. Nevertheless we remind that it can easily lose accuracy in presence of large sudden volatility movements. Jumps that are not detected are generally quite small. Despite the jump intesity is constant, when the parameters of a univariate Hawkes process are estimated on detected jumps we statistically find significant self excitation effects (model 2). Nonetheless, such effects disappear as soon as we allow the baseline jump intensity to depend on the volatility level (model 4 in the paper). The experiment shows that this approach allows to take properly into account the effects of detection errors.

Table A1. Performances of the statistical test on simulated data. The nominal size is 0.005 for the m-LM test and 0.01 for the s-CPR.

	m-LM	s-CPR	m-LM ∩ s-CPR
Power	68.9%	60.4%	60.2%
Size	1.0%	1.8%	0.2%
avg. size non-detected jumps	0.25%	0.32%	0.32%

Appendix 2. The intraday volatility pattern

It is well established that the stock market volatility tends to be higher at the beginning and at the end of each trading day (see Wood, McInish, and Ord 1985; Harris 1986 for seminal contributions). Therefore, it is essential to take into account the intraday volatility pattern for the purpose of jumps identification (see also Boudt, Croux, and Laurent 2011). Several methods have been proposed in the literature to estimate the intraday volatility correction factor. As an example, Taylor and Xu (1997) use the simple estimator $\hat{\zeta}^2_{TX,i}$ based on the realized volatility measure:

$$\hat{\zeta}^2_{TX,i} = \frac{M \sum_{t=1}^{T} r^2_{t,i}}{\sum_{t=1}^{T} \sum_{i=1}^{M} r^2_{t,i}} \tag{A5}$$

Andersen and Bollerslev (1997) propose a more sophisticated technique called flexible Fourier function (FFF) that is based on the following regression:

$$\log |r_{t,i}| - c = \mathbf{x}_i' \theta + \epsilon_{t,i} \tag{A6}$$

where c corresponds to the mean of the log absolute value of a standard normal random variable and

$$\mathbf{x}_i' \theta = \sum_{q=0}^{Q} \sigma_t^q \left[\mu_{0,q} + \mu_{1,q} \frac{i}{N_1} + \mu_{1,q} \left(\frac{i}{N_2} \right)^2 + \sum_{l=1}^{D} \lambda_{l,q} I_{\{i=d_l\}} + \sum_{p=1}^{P} \left(\gamma_{p,q} \cos \frac{p \cdot i \cdot 2\pi}{M} + \kappa_{p,q} \sin \frac{p \cdot i \cdot 2\pi}{M} \right) \right] \tag{A7}$$

where $\theta = [\mu_{0,q}, \mu_{1,q}, \lambda_{l,q}, \gamma_{p,q}, \kappa_{p,q}]$ is a parameter vector, σ_t is a measure of the daily volatility level, $N_1 = (N+1)/2$ and $N_2 = (N+1)(N+2)/6$. The regression is estimated by OLS and the intraday volatility corrector is obtained as

$$\hat{\zeta}^2_{FFF,i} = \frac{M \exp\left(2\mathbf{x}_i' \theta\right)}{\sum_{i=M}^{M} \exp\left(2\mathbf{x}_i' \theta\right)} \tag{A8}$$

Importantly, neither the estimators described above nor the method proposed by Bormetti et al. (2015) are robust to the presence of price jumps. So, if price discontinuities are concentrated in specific periods within the trading day, they may induce some distortions in the estimate of the intraday volatility corrector and consequently in the instantaneous volatility measurement. The problem is discussed by Boudt, Croux, and Laurent (2011) who propose alternative parametric and non-parametric estimators. Let us first consider the standardized returns defined as follows:

$$\bar{r}_{t,i} = \frac{r_{t,i}}{\sqrt{BV_t/M}}$$

the shortest half scale estimator is

$$ShortH_i = 0.741 \ \min \left\{ \bar{r}_{(h),i} - \bar{r}_{(1),i}, \ldots, \bar{r}_{(T),i} - \bar{r}_{(T-h+1),i} \right\}$$

Table A2. Hawkes model parameters estimated on simulated data.

		m-LM	s-CPR	Intersection
model 1	θ	$1.77 \cdot 10^{-3***}$	$1.57 \cdot 10^{-3***}$	$1.53 \cdot 10^{-3***}$
		$(1.44 \cdot 10^{-5})$	$(1.31 \cdot 10^{-5})$	$(1.29 \cdot 10^{-5})$
	log L	−79359.8	−71847.4	−70393, 1
model 2	θ	$1.41 \cdot 10^{-3***}$	$1.18 \cdot 10^{-3***}$	$1.13 \cdot 10^{-3***}$
		$(5.94 \cdot 10^{-5})$	$(4.44 \cdot 10^{-5})$	$(4.32 \cdot 10^{-5})$
	γ	$3.18 \cdot 10^{-4***}$	$4.37 \cdot 10^{-4***}$	$4.16 \cdot 10^{-4***}$
		$(7.72 \cdot 10^{-5})$	$(7.34 \cdot 10^{-5})$	$(6.80 \cdot 10^{-5})$
	K	$6.49 \cdot 10^{-5***}$	$1.09 \cdot 10^{-4***}$	$1.09 \cdot 10^{-4***}$
		$(1.21 \cdot 10^{-5})$	$(1.40 \cdot 10^{-5})$	$(1.37 \cdot 10^{-5})$
	log L	−79327.6	−71779.1	−70321.3
model 4	a	−9.23***	−10.2***	−10.4***
		$(1.19 \cdot 10^{-1})$	$(1.27 \cdot 10^{-1})$	$(1.28 \cdot 10^{-1})$
	b	$-2.04 \cdot 10^{-1***}$	$-2.66 \cdot 10^{-1***}$	$-2.75 \cdot 10^{-1***}$
		$(8.33 \cdot 10^{-3})$	$(8.83 \cdot 10^{-3})$	$(8.92 \cdot 10^{-3})$
	γ	–	–	–
		–	–	–
	K	–	–	–
		–	–	–
	log L	−79077.66	−71420.9	−69950.1

where T is the total number of observations, $h = \lfloor T/2 \rfloor$ is the floor of $T/2$ and $\bar{r}_{(j),i}$ are the order statistics of $\bar{r}_{j,i}$. Then the corresponding correction factor is

$$\hat{\zeta}^2_{ShotH,i} = \frac{M\, ShortH_i^2}{\sum_{i=1}^{M} ShortH_i^2}$$

A more efficient non-parametric corrector is the weighted standard deviation estimator that assigns no weight to the largest observations after scaling by $\hat{\zeta}_{ShortH,i}$:

$$WSD_i^2 = 1.081 \frac{M \sum_{t=1}^{T} \omega_{t,i}\, \bar{r}_{t,i}^2}{\sum_{i=1}^{M} \omega_{t,i}}$$

where $\omega_{t,i} = \omega(\bar{r}_{t,i}/\hat{\zeta}_{ShortH,i})$ and $\omega(z) = 1$ if $z^2 \leq 6.635$ and 0 otherwise

$$\hat{\zeta}^2_{WSD,i} = \frac{M \cdot WSD_i^2}{\sum_{i=1}^{M} WSD_i^2} \tag{A9}$$

The parametric method proposed by Boudt, Croux, and Laurent (2011) represents a modification of the FFF estimator. To see this, consider the residuals

$$e^{WSD}_{t,i} = \log |r_{t,i}| - c - \log \hat{\zeta}_{WSD,i}$$

and define the negative likelihood function as

$$\rho_{ML}(z) = -0.5 \log\left(\frac{2}{\pi}\right) - z - c + 0.5 \exp\{2(z+c)\}$$

and the weights as

$$\omega_{t,i} = \begin{cases} 1 & \text{if } \rho_{ML}\left(e^{WSD}_{t,i}\right) \leq 3.36 \\ 0 & \text{otherwise.} \end{cases}$$

Then the maximum likelihood parameters are estimated as

$$\theta_{ML} = \min_{\theta} \frac{\sum_{t,i} \omega_{t,i} \rho_{ML}\left(\epsilon_{t,i}\right)}{\sum_{t,i} \omega_{t,i}}$$

where $\epsilon_{t,i}$ is calculated from a regression of the type (A6) and the truncated maximum likelihood (TML) corrector is given by Equation (A8).

Figure A1 shows the WSD and the TML volatility correctors computed on our sample. Generally speaking, the TML estimator is more efficient and also generates smoother patterns, but it fails to capture discontinuities. Therefore, we disregard the TML corrector for some specific time intervals as the one around 10:00 EST where the S&P 500 deviates from a standard U-shaped pattern and exhibits a peak due to the documented news announcements mentioned in the discussion of our results of the jump identification process; analogously the TML corrector is replaced around 14:25 CET when the Euro Stoxx 50 intraday volatility spikes because of the beginning of pre-negotiations in the U.S. In general, the intraday volatility of the Euro Stoxx 50 exhibits a strong dependence on the market activity in U.S. and Figure A1 illustrates the three different patterns observed depending on the operating time of the NYSE. The right top panel displays the pattern for a common trading day, i.e. when the Frankfurt Stock Exchange (FSX) electronic trading starts at 9:00 CET and closes at 17:30, while the NYSE opens at 15:30 CET and closes at 22:00 CET (respectively 9:30 and 16:00 EST). The overlapping period between these markets can vary based on changes resulting from the non-simultaneous adoption of the daylight saving time which generates short periods characterized by a different volatility pattern. In the left bottom panel we represent the shape of the volatility correctors for periods when the NYSE opens one hour earlier w.r.t. the CET due to the different adoption of the daylight saving time in the two regions. This anomaly involves a small number of trading days (117 out of 1691) and the WSD estimates are extremely noisy, thus we fully rely on the TML estimates except for the first 5 minutes interval when volatility is extremely large. Finally, there is a small set of days in which the FSX market is operating normally but the NYSE remains closed (only 44 days in the whole sample including some long weekends and national holidays in U.S.). The volatility pattern of the Euro Stoxx appears L-shaped during these periods as displayed by the right bottom panel in Figure A1.

Appendix 3. Forecasting the integrated volatility

In this Section we discuss some details on the volatility proxy used in the Hawkes process estimation. The objective is to provide accurate estimates of the integrated volatility on each trading day t using the previously available information. The aim of this approach is to circumvent some endogeneity issues which may arise if the integrated volatility is calculated subtracting the contribution of jumps from the quadratic variation introducing therefore some dependence between the volatility estimates and the price jumps occurred in the same period. The dependent variables that we want to model are the integrated volatilities of the Euro Stoxx 50 ($IV_{EU,t}$) and of the S&P 500 ($IV_{EU,t}$). Let $r_{l,t}$ denote the close to close log-return on day t while $J_{l,t}$ is the absolute contribution

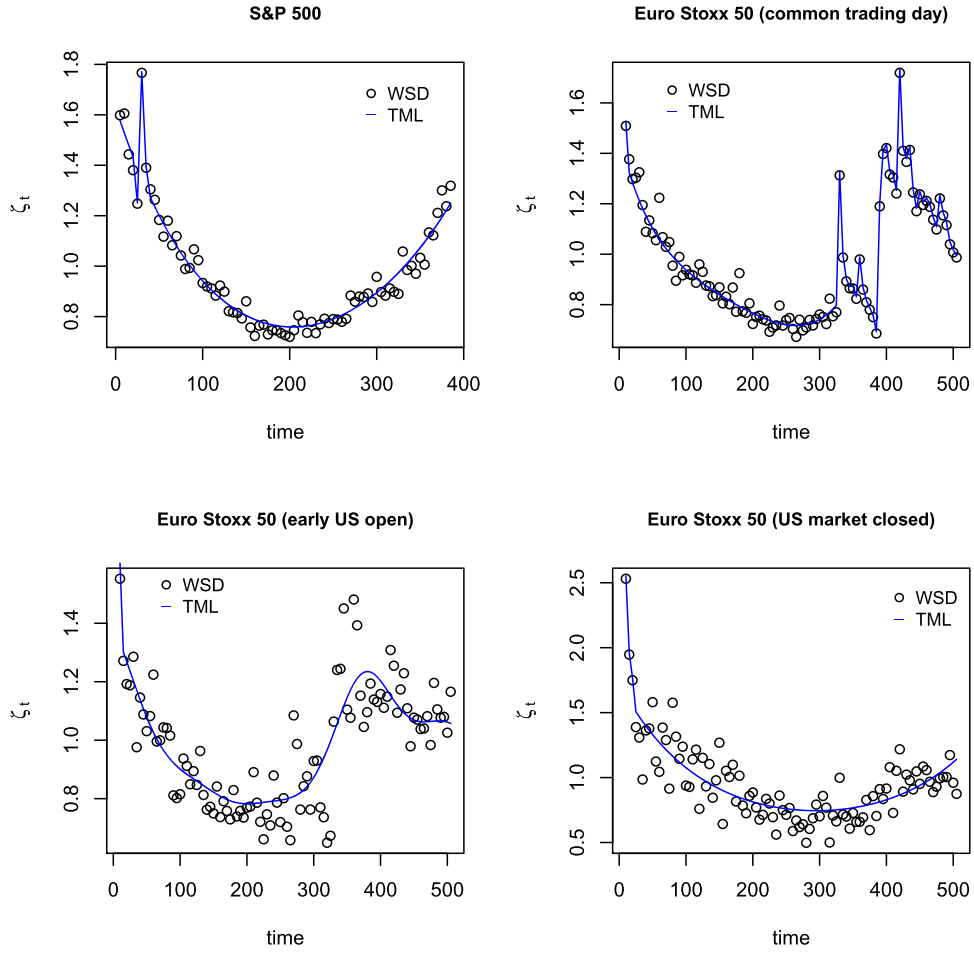

Figure A1. The blue line labeled as TML is the correction adopted in our study and it is constructed using a mixed approach: for the points lying in the neighborhood of discontinuities the TML estimator is substituted by the WSD.

of jumps to the quadratic variation. More specifically the integrated volatility is calculated as the average variance of the intraday log-returns that are not identified as jumps:

$$IV_{l,t} = \frac{M}{M - \sum_{i=1}^{M} Jump_{t,i}} \sum_{i=1}^{M} r_{t,i}^2 \left(1 - Jump_{t,i}\right)$$

where $Jump_{t,i}$ is the jump indicator taking the value 1 each time that a jump is identified and zero otherwise. Clearly, this method produces distinct volatility measures for each different jump identification method. Our approach is based on a bivariate extension of the LHAR-C-CJ regression of Corsi and Renò (2012), i.e. a parsimonious regression of the HAR type (introduced by Corsi 2009) which also includes lagged leverage effects and jumps in a way similar to Clements and Liao (2017). We propose a straightforward bivariate extension that is able to capture the cross market effects. As an example, for the Euro Stoxx 50, the regression reads as follows:

$$\begin{aligned}\log IV_{EU,t+1} = {} & c + \beta_1 \log IV_{EU,t} + \beta_2 \log IV_{EU,t}^{(5)} + \beta_3 \log IV_{EU,t}^{(22)} + \beta_4 \log\left(1 + J_{EU,t}\right) + \beta_5 \log\left(1 + J_{EU,t}^{(5)}\right) + \beta_6 \log\left(1 + J_{EU,t}^{(22)}\right) \\ & + \beta_7 r_{EU,t}^{-} + \beta_8 r_{EU,t}^{(5)-} + \beta_9 r_{EU,t}^{(22)-} + \beta_{10} \log IV_{US,t} + \beta_{11} \log IV_{US,t}^{(5)} + \beta_{12} \log IV_{US,t}^{(22)} + \beta_{13} \log\left(1 + J_{US,t}\right) \\ & + \beta_{14} \log\left(1 + J_{US,t}^{(5)}\right) + \beta_{15} \log\left(1 + J_{US,t}^{(22)}\right) + \beta_{16} r_{US,t} + \beta_{17} r_{US,t}^{(5)-} + \beta_{18} r_{US,t}^{(22)-}\end{aligned}$$

where for a generic observable X we have:

$$X^{-} = \min\left(X, 0\right)$$

Table A3. MLE of bivariate LHAR-C-CJ process.

	ESTX			S&P 500		
	m-LM	s-CPR	m-LM ∩ s-CPR	m-LM	s-CPR	m-LM ∩ s-CPR
c	−1.33***	−1.44***	−1.48***	−1.53***	−1.72***	−1.73***
	(0.20)	(0.21)	(0.20)	(0.20)	(0.20)	(0.20)
IV_{US}	0.22***	0.24***	0.23***	0.44***	0.39***	0.39***
	(0.03)	(0.03)	(0.03)	(0.03)	(0.03)	(0.03)
$IV_{US}^{(5)}$	−0.10	−0.09	−0.09	0.24***	0.27***	0.27***
	(0.05)	(0.06)	(0.06)	(0.05)	(0.05)	(0.06)
$IV_{US}^{(22)}$	−0.07	−0.10*	−0.10*	0.25***	0.27***	0.27***
	(0.05)	(0.05)	(0.05)	(0.05)	(0.05)	(0.05)
J_{US}	11.21	373.41	475.28	32.60	188.37	526.30
	(367.65)	(355.44)	(381.62)	(312.84)	(606.05)	(609.65)
$J_{US}^{(5)}$	374.63	495.97	299.76	186.61	−28.31	−505.50
	(647.56)	(1204.55)	(1276.56)	(804.68)	(1412.76)	(1472.98)
$J_{US}^{(22)}$	−1309.15	−3032.51	−2223.71	−1299.17	355.15	1418.30
	(1436.40)	(2858.22)	(2953.36)	(1439.30)	(2871.98)	(2913.64)
r_{US}^{-}	−1.05	−0.78	−0.97	−6.70***	−7.26***	−7.44***
	(1.61)	(1.76)	(1.74)	(1.96)	(2.07)	(2.08)
$r_{US}^{(5)-}$	0.79	−0.20	0.53	−12.19	−12.70	−12.81
	(5.61)	(6.06)	(6.01)	(6.41)	(6.72)	(6.57)
$r_{US}^{(22)-}$	25.98	26.96	29.41*	8.89	19.18	22.56
	(15.47)	(15.15)	(14.82)	(17.04)	(17.98)	(18.09)
J_{EU}	−299.77	−288.77	−297.08	−530.12*	−450.34	−400.91
	(264.21)	(265.17)	(273.65)	(259.97)	(311.68)	(339.78)
$J_{EU}^{(5)}$	−657.64	−722.77	−707.31	−1015.27	−1334.81	−1486.38
	(727.60)	(728.93)	(790.90)	(849.13)	(888.68)	(909.46)
$J_{EU}^{(22)}$	−352.97	−264.96	−108.15	−178.40	−569.12	−360.00
	(1252.21)	(1308.38)	(1318.49)	(1367.05)	(1455.09)	(1492.77)
IV_{EU}	0.25***	0.19***	0.19***	−0.01	−0.02	−0.02
	(0.04)	(0.04)	(0.04)	(0.04)	(0.04)	(0.04)
$IV_{EU}^{(5)}$	0.35***	0.38***	0.38***	0.00	0.02	0.02
	(0.05)	(0.05)	(0.05)	(0.05)	(0.06)	(0.06)
$IV_{EU}^{(22)}$	0.22***	0.24***	0.23***	−0.07	−0.09	−0.09
	(0.05)	(0.05)	(0.05)	(0.05)	(0.06)	(0.06)
r_{EU}^{-}	−12.60***	−13.60***	−13.26***	−10.52***	−10.28***	−10.05***
	(1.64)	(1.73)	(1.75)	(1.67)	(1.76)	(1.75)
$r_{EU}^{(5)-}$	−23.10***	−22.90***	−23.44***	−14.58*	−16.91**	−16.72**
	(5.01)	(5.20)	(5.19)	(6.18)	(6.32)	(6.31)
$r_{EU}^{(22)-}$	−34.97**	−35.51**	−36.17**	−31.36*	−37.80**	−37.79**
	(12.04)	(12.46)	(12.43)	(13.90)	(14.53)	(14.38)
R^2	0.81	0.79	0.79	0.85	0.84	0.84
obs.	1669	1669	1669	1652	1652	1652
RMSE	0.40	0.43	0.42	0.44	0.46	0.46

Notes: $^{***}p < 0.001$, $^{**}p < 0.01$, $^{*}p < 0.05$.
Estimates for the bivariate LHAR-C-CJ, robust to heteroskedasticity and autocorrelation. Standard errors in parentheses.

$$X_t^{(h)} = \frac{1}{h}\sum_{j=1}^{h} X_{t-h+1}$$

$$X^{(h)-} = \min\left(X^{(h)}, 0\right)$$

$$X^{-(h)} = \frac{1}{h}\sum_{j=1}^{h} \min\left(X_{t-h+1}, 0\right)$$

with h representing the order of the LHAR-C-CJ component.

The results shown in Table A3 are very similar under the alternative jump identification schemes adopted. For both indexes the strong volatility persistence is confirmed: the coefficients relative to the daily, weekly and monthly components are positive and significant. The persistence of the leverage effects is also relevant, especially for the Euro Stoxx 50 index. The main differences with respect to Corsi and Renò (2012) are found in the impact of jumps on continuous volatility which is generally insignificant in our regressions. This is probably due to the prevalence of crisis periods in our sample, when the effect of jumps is overwhelmed by a large continuous volatility component as already documented in the paper. Concerning volatility spillovers, we note a strong effect from U.S. to Europe with a lag of 1 day while the weekly component has a weak negative effect and the monthly component is not statistically significant. Importantly, we also notice a marked cross-leverage effect between Europe and U.S. that to the best of our knowledge is unprecedented in the literature and is probably mostly generated during the Euro Sovereign crisis, which suggests a possible direction for future research. The interdependence in volatility stems also from the cross correlation of the residuals that is over 40% under all jump identification methods.